AD-A069 131 WIGGINS (J H) CO REDONDO BEACH CALIF F/G 19/4
UNCERTAINTIES IN THE GROUND SHOCK ESTIMATION PROCESS.(U)
AUG 78 J D COLLINS, R D DANIELS, K B OVERBECK DNA001-77-C-0295
UNCLASSIFIED 77-1310 DNA-4769Z NL

| OF |
AD
A069131

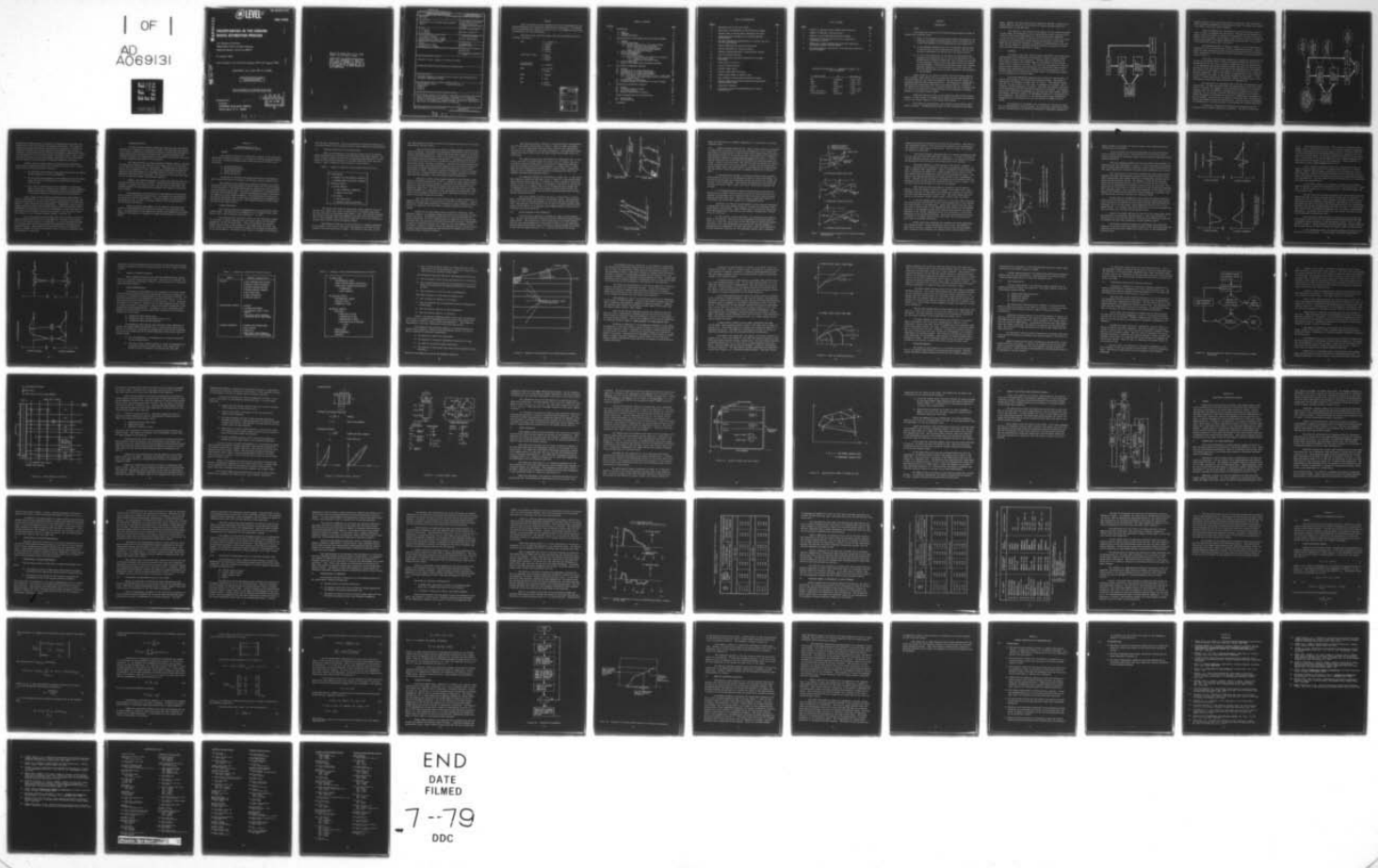

END
DATE
FILMED
7-79
DDC

DNA 4769Z

UNCERTAINTIES IN THE GROUND SHOCK ESTIMATION PROCESS

J.H. Wiggins Company
1650 South Pacific Coast Highway
Redondo Beach, California 90277

31 August 1978

Interim Report for Period 31 August 1977—31 August 1978

CONTRACT No. DNA 001-77-C-0295

THIS WORK SPONSORED BY THE DEFENSE NUCLEAR AGENCY
UNDER RDT&E RMSS CODE B344078464 Y99QAXSB04913 H2590D.

Prepared for
Director
DEFENSE NUCLEAR AGENCY
Washington, D. C. 20305

Destroy this report when it is no longer needed. Do not return to sender.

PLEASE NOTIFY THE DEFENSE NUCLEAR AGENCY, ATTN: TISI, WASHINGTON, D.C. 20305, IF YOUR ADDRESS IS INCORRECT, IF YOU WISH TO BE DELETED FROM THE DISTRIBUTION LIST, OR IF THE ADDRESSEE IS NO LONGER EMPLOYED BY YOUR ORGANIZATION.

UNCLASSIFIED

SECURITY CLASSIFICATION OF THIS PAGE *(When Data Entered)*

REPORT DOCUMENTATION PAGE		READ INSTRUCTIONS BEFORE COMPLETING FORM
1. REPORT NUMBER DNA 4769Z	2. GOVT ACCESSION NO.	3. RECIPIENT'S CATALOG NUMBER
4. TITLE *(and Subtitle)* UNCERTAINTIES IN THE GROUND SHOCK ESTIMATION PROCESS		5. TYPE OF REPORT & PERIOD COVERED Interim Report for Period 31 Aug 77—31 Aug 78 6. PERFORMING ORG. REPORT NUMBER 77-1310
7. AUTHOR(s) J. D. Collins R. D. Daniels K. B. Overbeck		8. CONTRACT OR GRANT NUMBER(s) DNA 001-77-C-0295 new
9. PERFORMING ORGANIZATION NAME AND ADDRESS J. H. Wiggins Company 1650 South Pacific Coast Highway Redondo Beach, California 90277		10. PROGRAM ELEMENT, PROJECT, TASK AREA & WORK UNIT NUMBERS Subtask Y99QAXSB049-13
11. CONTROLLING OFFICE NAME AND ADDRESS Director Defense Nuclear Agency Washington, D.C. 20305		12. REPORT DATE 31 August 1978 13. NUMBER OF PAGES 86
14. MONITORING AGENCY NAME & ADDRESS(if different from Controlling Office)		15. SECURITY CLASS *(of this report)* UNCLASSIFIED 15a. DECLASSIFICATION/DOWNGRADING SCHEDULE

16. DISTRIBUTION STATEMENT *(of this Report)*

Approved for public release; distribution unlimited.

17. DISTRIBUTION STATEMENT *(of the abstract entered in Block 20, if different from Report)*

18. SUPPLEMENTARY NOTES

This work sponsored by the Defense Nuclear Agency under RDT&E RMSS Code B344078464 Y99QAXSB04913 H2590D.

19. KEY WORDS *(Continue on reverse side if necessary and identify by block number)*

Nuclear Weapons Effects
Ground Shock
Airblast
Cratering
Uncertainty Analysis

20. ABSTRACT *(Continue on reverse side if necessary and identify by block number)*

A qualitative analysis of the effect of uncertainty on the free-field ground shock estimation process is presented. The approach is to examine the process as a modeling problem and examine each part so as to isolate uncertainties in the framework of the model problem. Qualitative assessments of the effects of various uncertainties are presented.

DD FORM 1 JAN 73 1473 EDITION OF 1 NOV 65 IS OBSOLETE

UNCLASSIFIED

SECURITY CLASSIFICATION OF THIS PAGE *(When Data Entered)*

PREFACE

While the results herein represent the authors' perspective on the addressed problem, many people have contributed to the effort. The authors wish to acknowledge the cumulative efforts of Dr. Erik Vanmarcke in the area of probability in Soils Engineering.

The authors also received helpful input and discussion from the following individuals:

WES	J.G. Jackson, Jr.
	J. Zelasko
	P. Hadala
	G. Baladi
	E. Jackson
Weidlinger, Assoc.	M. Baron
	I. Sandler
	I. Nelson
Civil/Nuclear Systems Corp.	J.L. Bratton
AFWL	G.W. Ullrich
	S. Melzer
CERF	C. Higgins
RDA	R. Port
DNA	E. Sevin
	G. Ullrich

TABLE OF CONTENTS

LIST OF ILLUSTRATIONS

LIST OF TABLES

CONVERSION FACTORS FOR U.S. CUSTOMARY TO METRIC (SI) UNITS OF MEASURE

To Convert From	To	Multiply By
bar	kilopascal	$2.000 \times 10^{+2}$
foot	meter	3.048×10^{-1}
inch	meter	2.540×10^{-2}
kiloton	terajoules	4.183
mile	meter	$1.609 \times 10^{+3}$
mile (nautical)	meter	$1.852 \times 10^{+3}$
pound-force/inch^2	kilopascal	6.894

SECTION I

INTRODUCTION

1. SCOPE

This study was initiated by the Defense Nuclear Agency in order to address the following issues:

- There is an increasing inquisitiveness about the presence of uncertainty throughout the ground shock process, and there is not a good understanding of the consequences of this uncertainty;
- In the proposed implementation of new land-based systems there is large variety in soil conditions and geology. How can this variety be considered and controlled in the design process?
- In view of the uncertainty in the output of ground shock measurements and simulations and in view of the variability in the determination of material properties, what accuracy is warranted in the individual steps of the ground shock estimation process? Are some elements of the process overworked where other elements need more emphasis, or is the uncertainty in some areas such that the computational error is small compared to the randomness of the problems?

These issues are of concern throughout the ground shock community which includes, among others, the soil properties analyst, the designer of the ground facility, the simulation modeller, and the oversight agents for research expenditure and system expenditure. The community is fragmented in addressing the uncertainty issues and in correlating efforts. Therefore, the objective of this study is to illuminate these issues and to analyze them in light of the offensive and defensive goals of the treatment of nuclear weapons by the Defense Nuclear Agency.

Resolving the above issues is far beyond the scope of this effort. However, it does attempt to systematically analyze the interacting uncertainties in the various elements of the ground shock process.

This study was an experiment, and intended to be primarily qualitative in nature. Consequently many areas are not considered in any great

depth. However, the effort does offer a systematic approach to defining research needs or evaluating the direction of current programs toward the maximum benefit to the DNA goals.

The authors of this report are not experts in most fields discussed in this study, and consequently, had to rely heavily on oral and written information from various participants in the DNA ground shock community. Visits were made to a number of agencies and contractors to acquire an understanding in the problem and to help develop the structure of the study. Hopefully the study will represent a consensus of understanding of the problems, and yet reveal by the system analysis approach the impacts of uncertainty and the relative importance of issues.

2. APPROACH

An extensive data base enables drawing conclusions and establishing relationships with a high degree of confidence. However, nuclear effects data does not support such an approach. The data base is limited by the small number of tests, the limited range of environments and the limited yields of the weapons in the tests. The library of high explosive tests improves nuclear prediction but necessarily is a limited data base extension. Therefore the consequences of the variabilities and uncertainties in the various elements of the ground shock system cannot be conclusively assessed by an investigation of available data.

This study emphasizes separating and tracing the uncertainties in each of the elements of the ground shock modeling process. The system is described by the sequence of steps shown in Figure 1. The modeller begins with the *real system* which, in this case, is composed of the weapon, the environment, and the propagation of energy. From this real system, *mathematical models* (representations) are created of elements of the system. For example, constitutive equations are developed for soil behavior under dynamic loading. Gas dynamic, structural dynamic, or hydrodynamic behavior is incorporated in other submodels. The second box in the diagram depicts these mathematical representations of the behavior of the real system, or elements of the system.

The synthesis of the models into a computation involves the *simulation* of the behavior of the real system. This simulation exercises the mathematical representations and should be structured to adequately reproduce or

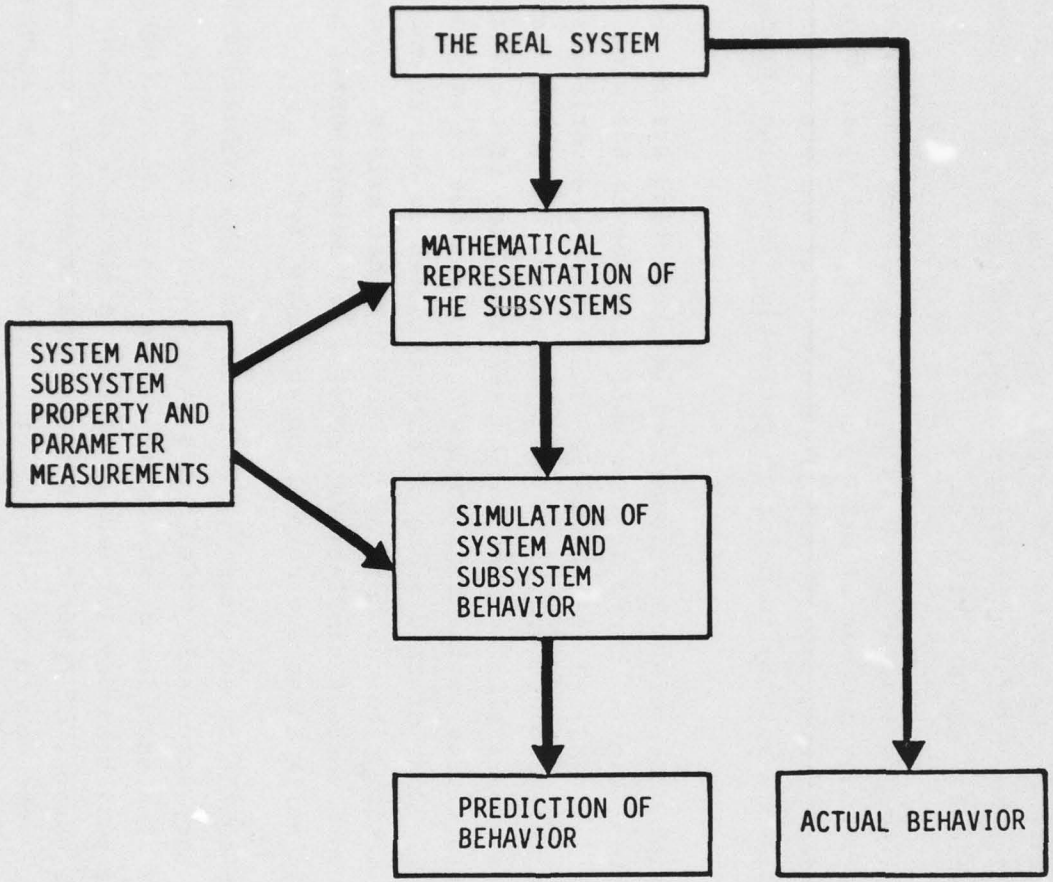

Figure 1. Representation of the Real System

predict behavior within the narrow frame of a particular test configuration. Thus the combined mathematical representations model the system, and simulation models a particular system response.

Both the mathematical representations and the simulation require input in order to represent the real system. The data may be responses of system elements or physical *measurements* of parameters for use in the mathematical representations. The process of acquiring the right data, making the correct measurements, and making appropriate interpretations, is in itself a very difficult science, and a little art.

The modeling process, as shown in Figure 1, is very convenient in separating out the various sources of error, uncertainty and bias. Figure 2 shows how these uncertainties come from different sources and are primarily due to breakdowns in the ability to maintain perfection in moving through the steps in Figure 1.

The initial uncertainties encountered in predicting system behavior are due to the system itself. There are variabilities due to the wide inhomogeneity of the soil and its in-situ properties; there are variabilities in the atmospheric and surface conditions which influence the shock characterization; there are variabilities due to the repeatability of the weapons; and there are variabilities in the behavior of structures due to varying mechanical properties. None of this group of uncertainties is due to modeling or measurement, but rather to the natural variability that exists. Consequently, if there were perfect simulations, models, and measurements, these variabilities would still exist and have to be accounted for.

The next source of uncertainty has to do with the mathematical representations. Do they accurately model the system behavior under the conditions of interest? For example, do the constitutive models of soil behavior represent the true soil behavior (assuming the soil properties are known perfectly) for the variety of dynamic conditions experienced in a nuclear weapon environment? The bounds of validity of a mathematical representation may be exceeded. The error due to modeling limitations cannot be simply described by standard statistical distributions. Uncertainty due to mathematical representation limitations needs to be evaluated on a case-by-case basis.

A simulation synthesizes the mathematical representations and available data to yield a prediction of behavior. The scale to which the

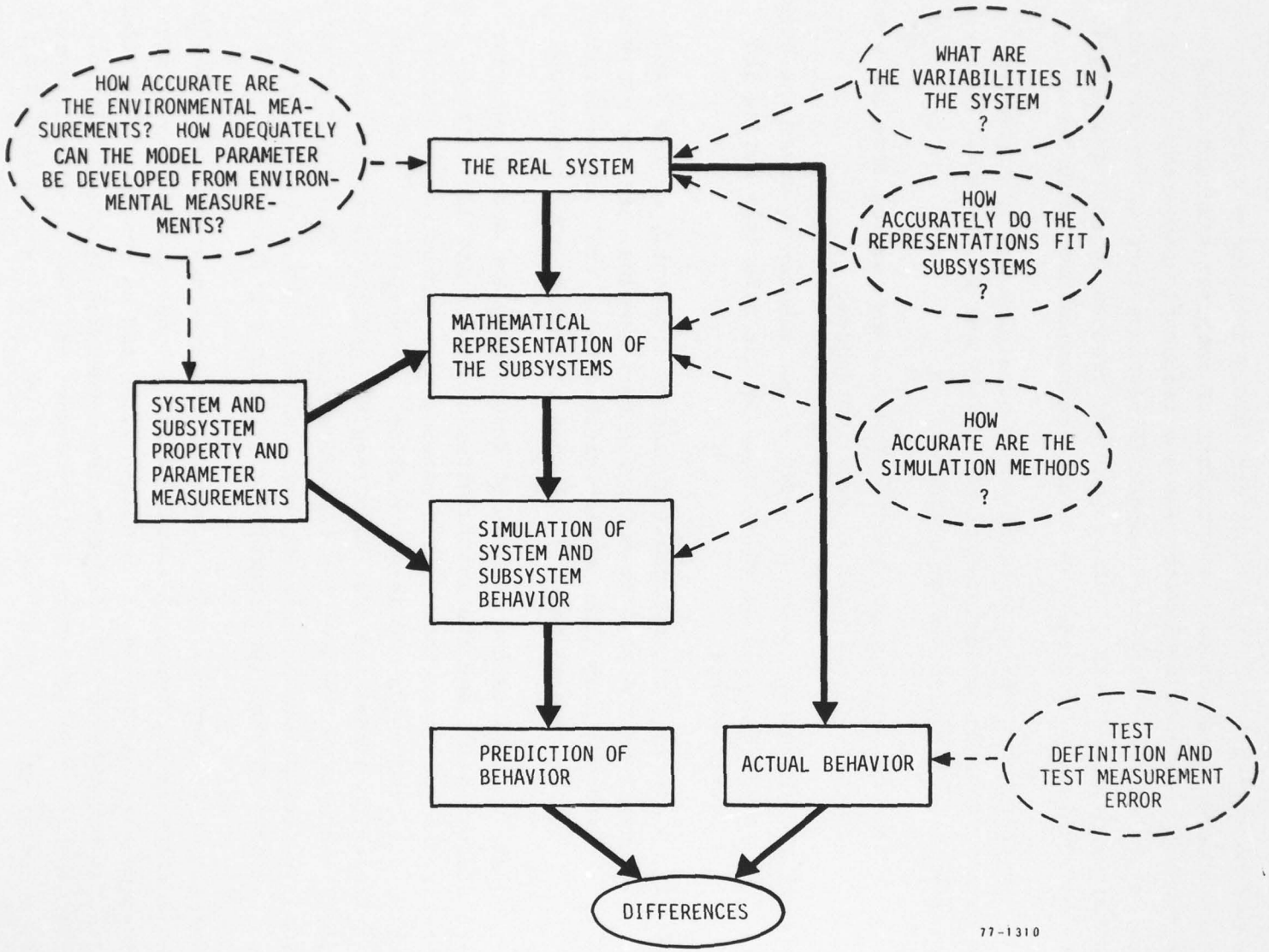

Figure 2. Uncertainty Consideration in the Prediction Process

mathematical representations are applied is constrained by practical considerations of data availability and economic limitations. The common assumption of homogeneous constant-thickness layers introduces a simulation limitation to abate the economic constraints of computer size and speed. Similarly, data availability limitations are frequently encountered in defining the properties of an increased number of distinct layers. Thus, variations within layers, varying layer depths, and changes in soil characteristics are commonly unincorporated and introduce simulation limitation.

Another source of uncertainties is obtaining and interpreting on-site data to develop parameters for the models and simulations. Several issues arise in deriving parameter estimates:

1) Do laboratory measurements on specimens removed from the ground account properly for in-situ influences?

2) Do the stress paths measured in the laboratory cover the stress paths that will be experienced by the materials during the nuclear event?

3) Since lack of repeatability occurs frequently in laboratory tests of the same or companion soil samples, are the parameters produced from these non-repeatable tests truly representative of the general behavior of that particular soil condition?

Lastly, there is the problem of determining the actual behavior. Tests are instrumented, but the instrumentation itself has limitations, and there are errors due to various causes ranging from mechanical or electrical behavior to data reduction and interpretation. Consequently, when trying to compare simulation output and test gage results, great care must be used to acknowledge the shortcomings of the test measurements so that improper interpretations are not placed on behavior and imposed on the simulation models. This subject will be discussed somewhat further in Section IV.

All of the uncertainties discussed thus far contribute to the differences between predictions and actual behavior. Because of the varying nature of the various sources of uncertainty, it can be concluded that there is no general model which will describe the uncertainties and account for these differences. The procedure in this report will be to categorize or classify a number of events and conditions and to treat the uncertainty problem separately in each case.

3. PROBLEM DEFINITION

For years, nuclear weapon response has generally been analyzed by deterministic as opposed to statistical methods. The magnitude and complexity of nuclear effects have dictated that effort be principally directed to establishing basic principles of behavior and correlating whatever data available, despite full acknowledgement of pervading uncertainties and variabilities throughout many aspects of the problem.

The sophistication of current simulation modeling efforts, and test and measurement programs, has advanced to the degree where it is now important to quantify the influence of uncertainty. The magnitude of uncertainty effects may be comparable to that of second-order effects and therefore appropriate emphasis/de-emphasis in expanded simulation efforts or test and measurement programs may be indicated. The ordering of priorities may therefore be an important output of uncertainty analysis.

However, the inherent complexity of uncertainty modeling makes its ultimate usefulness difficult to predict. Therefore this particular study attempts to address the problem in such a way that DNA can anticipate the possible benefits of future uncertainty analyses with regard to the ground shock problem.

The organization of this particular study emphasizes the development of mutually-consistent definitions of: the system; the representation; the simulation; and the measurements. The heavy emphasis on this modeling philosophy was made in order to provide a baseline for the discussion of various uncertainty models.

Numerous comments from members of the community have been incorporated in this document which offers an overview of the ground shock process. An understanding of the approaches, emphasis and assumptions of fellow members of the community is important to those concentrating on a particular aspect.

SECTION II

SYSTEM ANALYSIS OF THE GROUND SHOCK ESTIMATION PROCESS

4. GENERAL

As a starting point for an uncertainty analysis of the free-field ground shock estimation problem, it is useful to view the processes involved in context. Classical systems analysis techniques divide a problem into four areas:

1) System Description;
2) System Representation;
3) System Measurements;
4) System Simulation.

Following this technique facilitates specifying the assumptions made in each step within the process, and thereby isolating uncertainties.

When applied to the ground motion estimation process, the system description traces the phenomenology of ground motion due to nuclear weapon (or HE) detonation. The system representation specifies the various assumptions and simplifications made in arriving at mathematical representations of ground shock phenomenology. The system measurements involve establishing and measuring the key system parameters. The system simulation specifies the various assumptions made in exercising the mathematical representations to estimate the ground shock motion. The completed simulation model shows how the various steps interact.

5. SYSTEM DESCRIPTION

This section outlines the phenomenology of the free-field ground shock process. The material to be presented is of a summary nature, qualitative, and is taken primarily from References 1, 2, and 3.

The ground motions induced by nuclear (or HE) detonations depend on the amount of energy deposited into the ground surface and the energy propagation through the earth media. Thus, the magnitude and waveform depend upon the yield of the detonation, the height above (or below) the ground surface at which the detonation occurs, and the physical properties of the ground medium. The material that follows is divided for convenience

into two major subsections: the first discusses the physical properties of the ground medium; and the second discusses energy deposition and propagation.

5.1 Physical Properties of the Ground Medium

There are two aspects of the physical properties of the ground medium that principally influence the free-field ground shock process. The first of these is the stratification of subsurface earth materials, and the second is the mechanical behavior of the earth materials within each substratum. Table 1 summarizes the discussion in this section.

Table 1. Summary of Important Ground Medium Characteristics

- STRATIFICATION
  - NUMEROUS TYPES AND SUBCLASSES OF MATERIALS
  - INTERFACES RANGE FROM UNIFORM TO IRREGULAR
- MECHANICAL BEHAVIOR
  - DISCRETE PARTICLES
    - LOCAL IRREVERSIBLE DEFORMATIONS
    - COMPLEX STRESS/STRAIN
  - VOID SPACES
    - MULTI-PHASE SYSTEM
    - TRANSITION CHANGES BETWEEN PHASES

The typical stratification means that a great number of earth materials, e.g., sand, silt, clay, up through soft to extremely hard rocks, may come into play in the ground shock problem. Also, the interfaces between the various strata may range from moderately uniform (for soil-like materials) to very irregular (for the rock-like materials) due to the influence of factors such as folds, faults and bedding planes.

The mechanical behavior of earth materials is strongly influenced by two factors. The first is that many earth materials, typified by sand, consist of discrete particles of matter. The second is that most, if not

all, earth materials contain significant void spaces taken up by air or water depending on the water table.

The particulate nature of some soil types produces a potential for large, non-linear, irreversible and anisotropic deformations within an assemblage of individual particles. Plastic flow within the crystalline structure of the individual particles can occur in the vicinity of contact points without visibly altering the shape of the particles. Slippages at points of contact between particles can occur as particles reposition among one another and thereby acquire new sets of neighbors. The ease with which particles can slip on one another, and therefore the complexity of stress/strain behavior, will depend on present stress/strain levels and previous stress history within the soil mass. Similarly, compressive loadings are likely to produce large strains. Slippages between particles can produce strains much larger than those which develop in the continuum by crystal deformation.

Inability to resist large tensile stresses is still another consequence of the particulate nature of soils. Sands and gravels would normally be able to resist no tensile stresses. Certain soils, with a degree of cementation, show some resistance but normally only to the extent of a few pounds per square inch. An intact chunk of hard rock may resist very large tensile stresses but a large mass of even the hardest rock may exhibit relatively small resistance because of the almost inevitable existence of networks of fissures through the rock mass.

Also, the resistance of a particulate mass to shear deformation is generally much less than its resistance to compressive deformation. Large resistance to volume change relative to resistance to shear deformation characterizes all materials, but this effect is greatly amplified in soil-like systems.

Because of the multi-phase nature of most soil materials, their mechanical behavior is extremely complex and sensitive to the amount of water filling the pores. The mechanical properties of saturated materials will exhibit sensitivity to rate of loading that will depend on the relative ease with which the pore water can move within the mineral structure. Compression of partially saturated materials will cause the air to be absorbed in the pore water. Similarly, factors such as the compressibility of the pore water or phase transitions accompanying high pressures and temperatures can significantly affect mechanical behavior.

Some important general features of the stress/strain relationships for soils are shown qualitatively in Figure 3, which is taken from Reference 3. The left-hand graph shows the typical form for the stress/strain relationship for hydrostatic or confined compression. The right-hand curves present the typical shear stress and volume change versus shear strain relationships.

The important features of the behavior in compression are: 1) initially, the curve is concave toward the strain axis; 2) finally, the curve is concave toward the stress axis; 3) one cycle of loading and unloading leads to a residual strain and is accompanied by an energy loss; 4) subsequent cycles of loading and unloading produce similar curves, although the residual strain increment and the energy loss associated with each cycle gradually decrease with successive cycles.

The important features of the behavior in shear are: 1) the curves for loading are concave to the strain axis; 2) there is a limit beyond which shear stresses cannot increase; 3) a change in volume, generally a volume decrease, occurs as the shear stress is increased; 4) one cycle of loading and unloading leads to a residual strain and is accompanied by an energy loss; 5) subsequent cycles of loading and unloading produce similar curves, but the residual strain increment and the energy loss decreases during the next several load-unload cycles.

Rock is as complex a material as soils, in that rock is, in general, a non-homogeneous, anisotropic, discontinuous medium. The mechanical behavior of rock is strongly dependent on the rock type and geological history. The potential also exists for rock to react to nuclear (or HE) stress waves by block motion, or by slipping along bedding planes, rather than reacting as an elastic-like solid.

5.2 Energy Deposition and Propagation

This discussion separately considers two types of energy deposition. The next two subsections emphasize airblast-induced and direct-induced ground motion. The distinction is that ground motion is airblast-induced when the only energy deposition to the ground surface is by air shock while direct-induced ground motion arises from energy coupling between the ground surface and the weapon materials, i.e., explosive particles and casing.

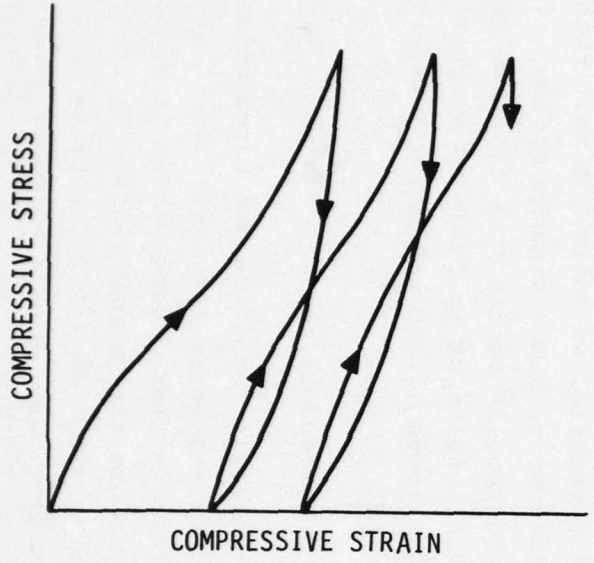

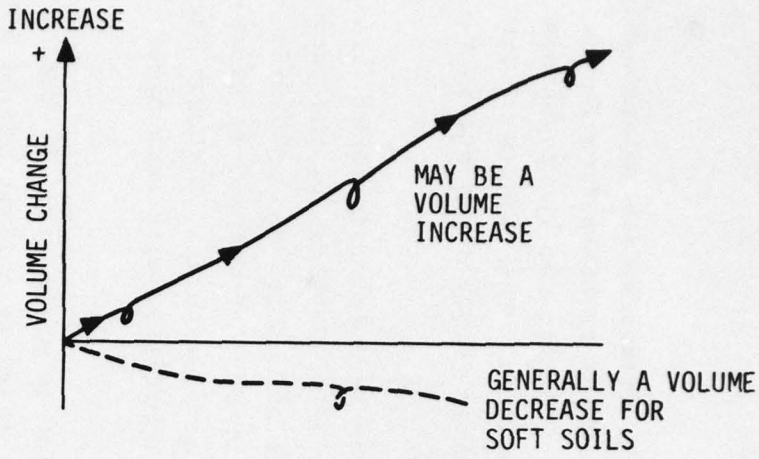

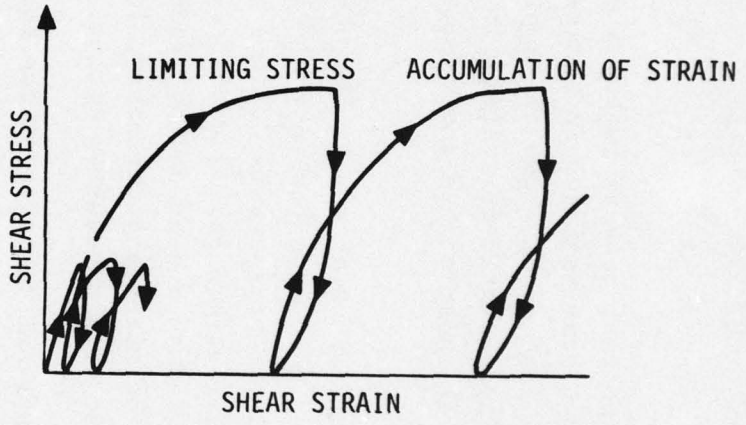

77-1310

Figure 3. General Forms of Stress Strain Relations for Soils

While this delineation is somewhat cumbersome, it is convenient to the discussion at hand.

5.2.1 Airblast-Induced Ground Motion. When a nuclear weapon is detonated at heights such that there is no more than a compaction crater formed, the only source of ground motion is the air shock which imposes normal pressures and horizontal shears on the ground surface. The ground motion induced by this process is generally termed airblast-induced ground motion. Airblast-induced ground motions are divided into two regions of phenomenological behavior. Close to the ground zero, the airblast velocity exceeds the velocity of the compression wave in the soil medium. In this, the so-called superseismic region, early time ground motion is characterized by a sharply downward and outward initial motion that is commonly referred to as the "air-slap."

As the blast wave expands, its velocity decreases and eventually falls below the velocity of the compression waves in the ground medium. At this point motions that are transmitted through the ground just precede the arrival of the airblast wave. This defines the beginning of the so-called "surface outrunning" region, where the initial ground motion precedes the air-slap.

In a homogeneous medium, where the earth material exhibits the properties of an elastic solid, the moving front of the airblast wave will generate a longitudinal and a transverse wave in the solid called the compression and shear Mach waves. Figure 4, which is taken from Reference 1, illustrates the airblast wave system for a homogeneous medium.

Initially, the velocity of disturbance is very large and generates a superseismic blast wave system (Figure 4a) in which no disturbance propagates ahead of the airblast. Rapid changes occur in stress and particle velocities accompanied by large vertical and outward accelerations, referred to as the "air-slap."

As the airblast velocity decreases, the compression wave advances ahead of the airblast. This yields the transseismic wave system shown in Figure 4b. Shear wave velocities are less than those of associated compression waves, and in the transseismic wave system the airblast passage is bracketed by the compression and shear Mach waves. This region defines the surface outrunning condition for the homogeneous medium since a wavefront

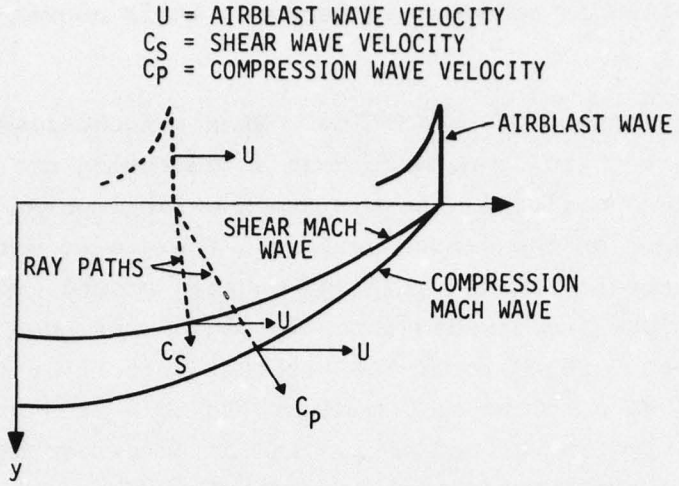

(a) SUPERSEISMIC AIRBLAST WAVE SYSTEM

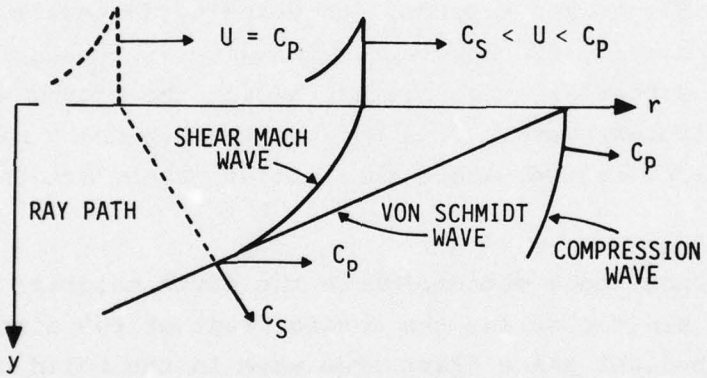

(b) TRANSSEISMIC AIRBLAST WAVE SYSTEM

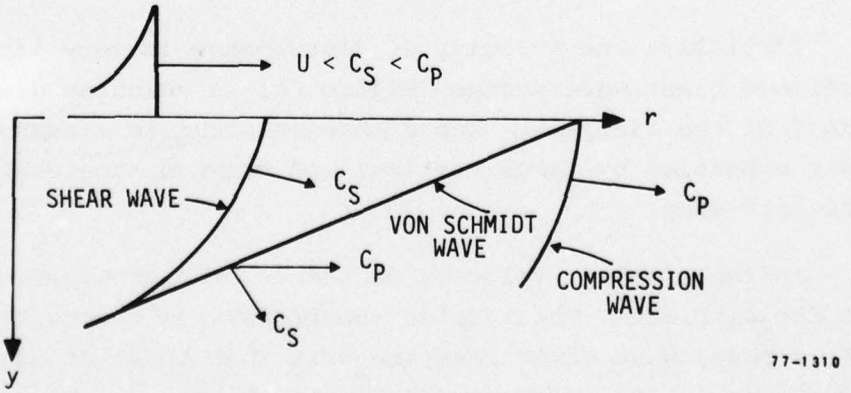

(c) SUBSEISMIC AIRBLAST WAVE SYSTEM

Table 4. Underground Wave Systems Due to Airblast-Induced Ground Motion

transmitted through the ground arrives ahead of the airblast. Note that in the transseismic system a third wave has been created by the interaction of the compression wave with the free surface. This is a shear wave called a von Schmidt or "head wave."

The airblast becomes subseismic when its velocity decreases so much that it lags behind the shear Mach wave (Figure 4c). In both the transseismic and subseismic regions, the initial disturbance is an upward and outward ground movement which arrives at the surface prior to the airblast.

This same sequence of events occurs in the case of a layered medium. Determining the incidence of the surface outrunning condition, however, is somewhat more complicated. Figure 5, presented in both References 1 and 2, illustrates an example of a raypath diagram for the case of a two-layer medium where the compression wave velocity increases with depth. Raypaths in the superseismic region are always straight lines in homogeneous strata. Elements of the wave move in the direction of the raypath with the compression wave velocity and move horizontally with a velocity equal to the airblast velocity at the point of origin of the raypath.

When the wave front intercepts an interface, such as shown in Figure 5, where the seismic velocity is greater in the lower layer than in the upper, a portion of the energy is reflected and a portion is refracted into the substratum according to Snell's law. The latter energy does not return to the surface unless a deeper higher velocity layer is present.

A ray will become totally refracted in a direction which parallels the interface when the airblast velocity first becomes equal to the compression wave velocity of the substratum. Energy then travels along the interface with a velocity equal to the compression wave velocity in the sublayer resulting in the sequence of wave front diagrams such as shown in Figure 5. Emergence at the surface (defined by Point G in the Figure), is the first appearance of the outrunning waveform. Since the initial particle velocity is always in a direction normal to the wave front, the initial motion is again seen to be upward and outward.

Weapon yield also influences the incidence of surface outrunning. The distance at which a given overpressure level occurs, and therefore a given shock velocity, increases with weapon yield to the one-third power. Thus, as weapon yield increases, the emergence point moves farther out. A

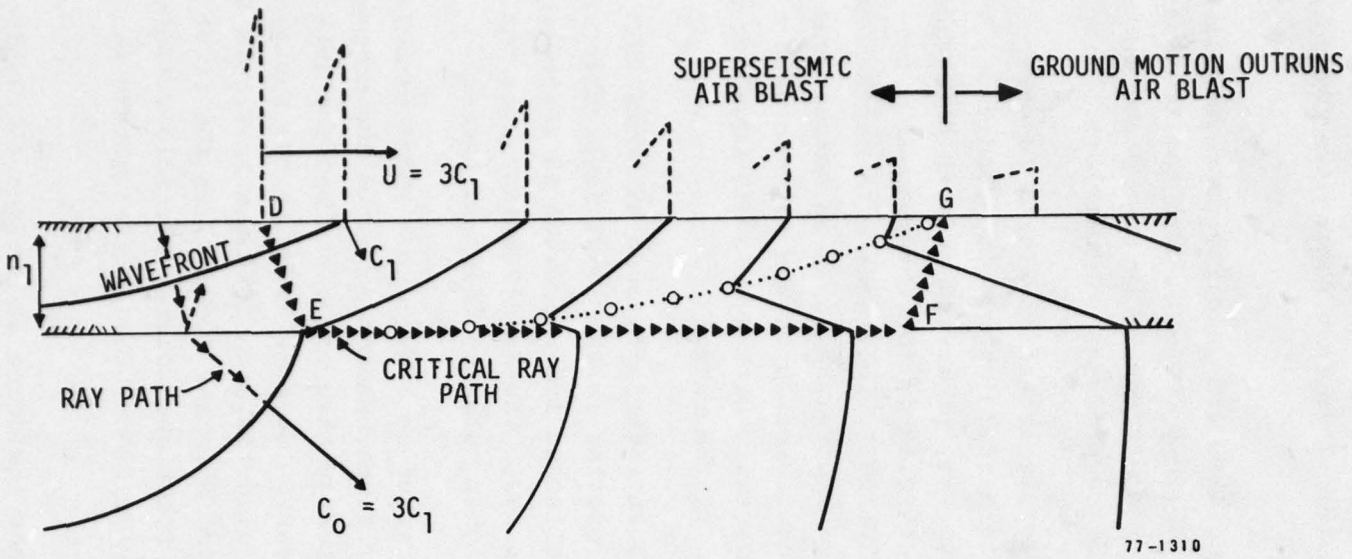

U = AIRBLAST VELOCITY

C_1 = COMPRESSION WAVE VELOCITY IN THE UPPER LAYER

C_0 = COMPRESSION WAVE VELOCITY IN THE SUBLAYER

Figure 5. Ray Path Diagram for Determination of Critical Ray Path for Two Layer Medium

similar analysis can be done for multiple layers, but refraction along all interfaces must be analyzed.

Up to this point, we have only discussed the early near-surface airblast-induced ground motion. The determination of the later time motions is complicated by non-linear elastic plastic behavior exhibited by most geologic materials.

Most soil materials exhibit the type of uniaxial strain/stress relationship that was illustrated in Figure 3. This relationship is characterized by concave downward behavior exhibited at small strains followed by concave upward behavior as the strain increases and by hysteresis upon cycling.

The implications of this type of behavior are best illustrated by considering single-layer homogeneous geology and focusing attention on the highly superseismic region where conditions of essentially uniaxial strain/stress are approximately correct. The changes in slope of the uniaxial strain/stress curve mean that the wave front in the superseismic airblast region will be propagated at a different velocity than the wave peak. This means that the stress wave will become "softer" as the acceleration decreases with increasing depth. Also, the hysteresis exhibited in the loading and unloading cycle means that the medium will absorb energy and, therefore, that the peak stress level will decrease with increasing depth.

As the point of consideration moves toward the surface outrunning region, the later portions of the ground motion become increasingly complex since the motion is generated by stress waves that have been attenuated and "softened" due to the non-linear, energy-absorbing characteristics of the ground medium. In a layered site, the waveform will be even more complex because of reflections from the various surface layers.

Overall, horizontal and vertical motions in the superseismic region are expected to qualitatively resemble Figure 6. The early portions are dominated by the air-slap and then by reflections from underlying layers and by stresses that have been propagated at higher pressure levels.

The primary difference between the superseismic and outrunning waveforms is that the outrunning region waveform is more oscillatory than the essentially one-directional damped motion that occurs in the superseismic airblast region.

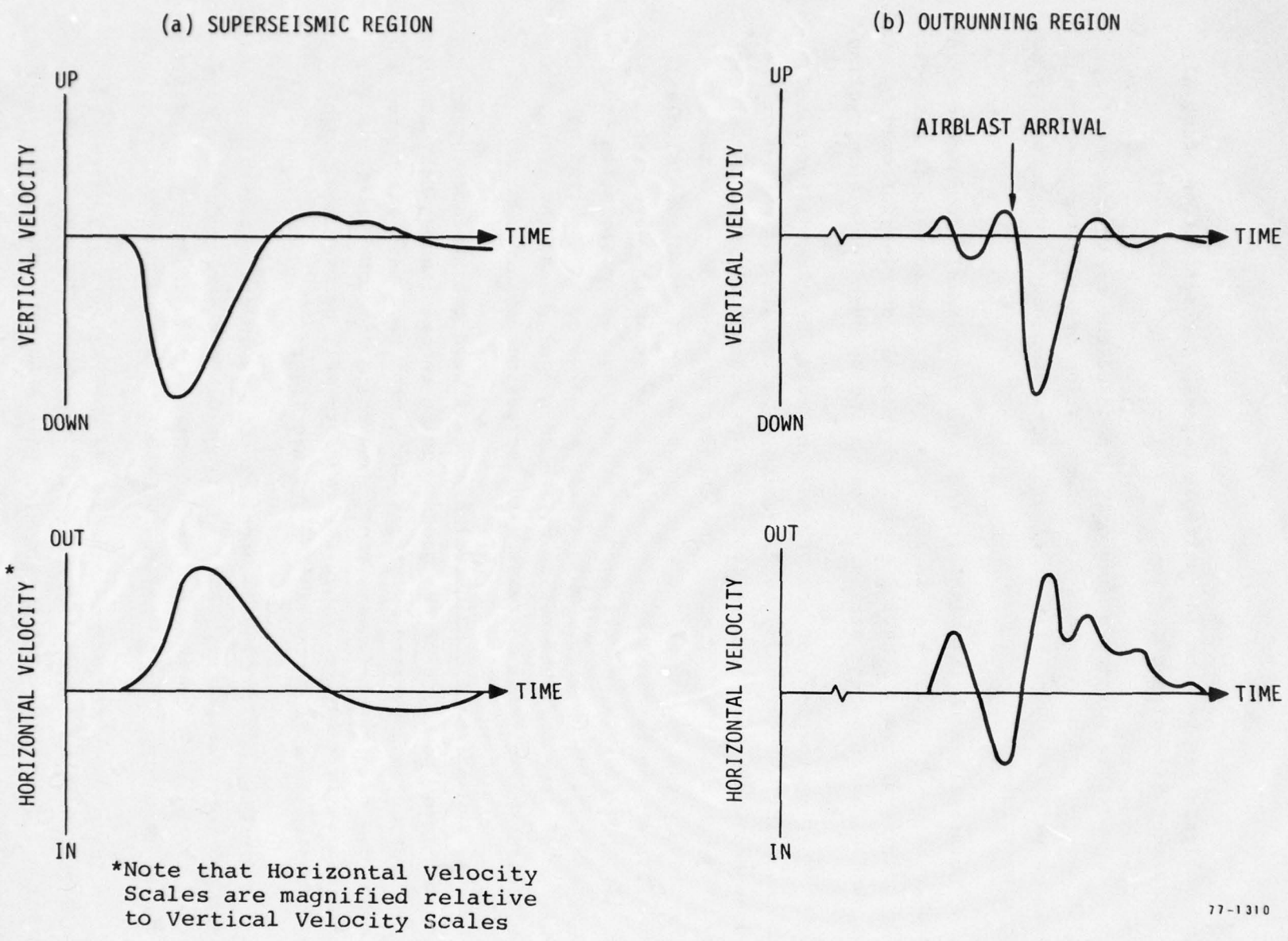

Figure 6. Typical Waveforms for Non-Cratering Bursts

5.2.2 Direct-Induced Ground Motion. When a weapon is detonated sufficiently close to the ground surface so as to cause an explosively excavated crater, a substantial portion of the weapon's energy is directly effective in producing pressures of multi-megabar magnitude and temperatures of the order of a million degrees in the ground immediately adjacent to the weapon case. The fraction of the energy transferred in this manner depends on the construction of the weapon and the soil properties. Energy deposited in this manner produces direct-induced ground motion.

At the extremes, ground motion due to a high altitude burst is purely airblast-induced, while from a deeply-buried charge, it is direct-induced. Between these extremes, ground motion can be induced by either or both mechanisms. However, the mechanisms exhibit vastly different attenuations, and therefore one or the other will dominate at a particular distance from the detonation. The two classifications are convenient for a discussion of ground shock phenomenology.

In the crater region, it is possible to identify four different zones of behavior in terms of the distortion of the original material. These are: 1) the fall back zone; 2) the rupture zone; 3) the plastic zone; and 4) the elastic zone.

The fall back zone consists of material that was disassociated and ejected into the air during cratering and has fallen back in the crater. In the rupture zone, the material, while severely fractured, sheared, and displaced has not been completely disassociated. The material in the rupture zone preserves some of the gross structural characteristics and compositional features which may have existed before cratering took place. In the plastic zone, the material is permanently displaced, but in a more or less homogeneous fashion. The plastic zone degrades into the elastic zone where no measurable permanent displacements occur.

Since the direct-induced energy is propagated solely through the earth medium, this motion will lag behind airblast-induced motion and lead to somewhat complex waveforms for the superseismic region. This is illustrated in Figure 7. These waveforms have been simplified to first illustrate the air-slap motion and then the upward and outward crater related motions.

In the outrunning region, the typical waveforms of Figures 6 and 7 are seen to be quite similar. In both cases, outrunning energy travels

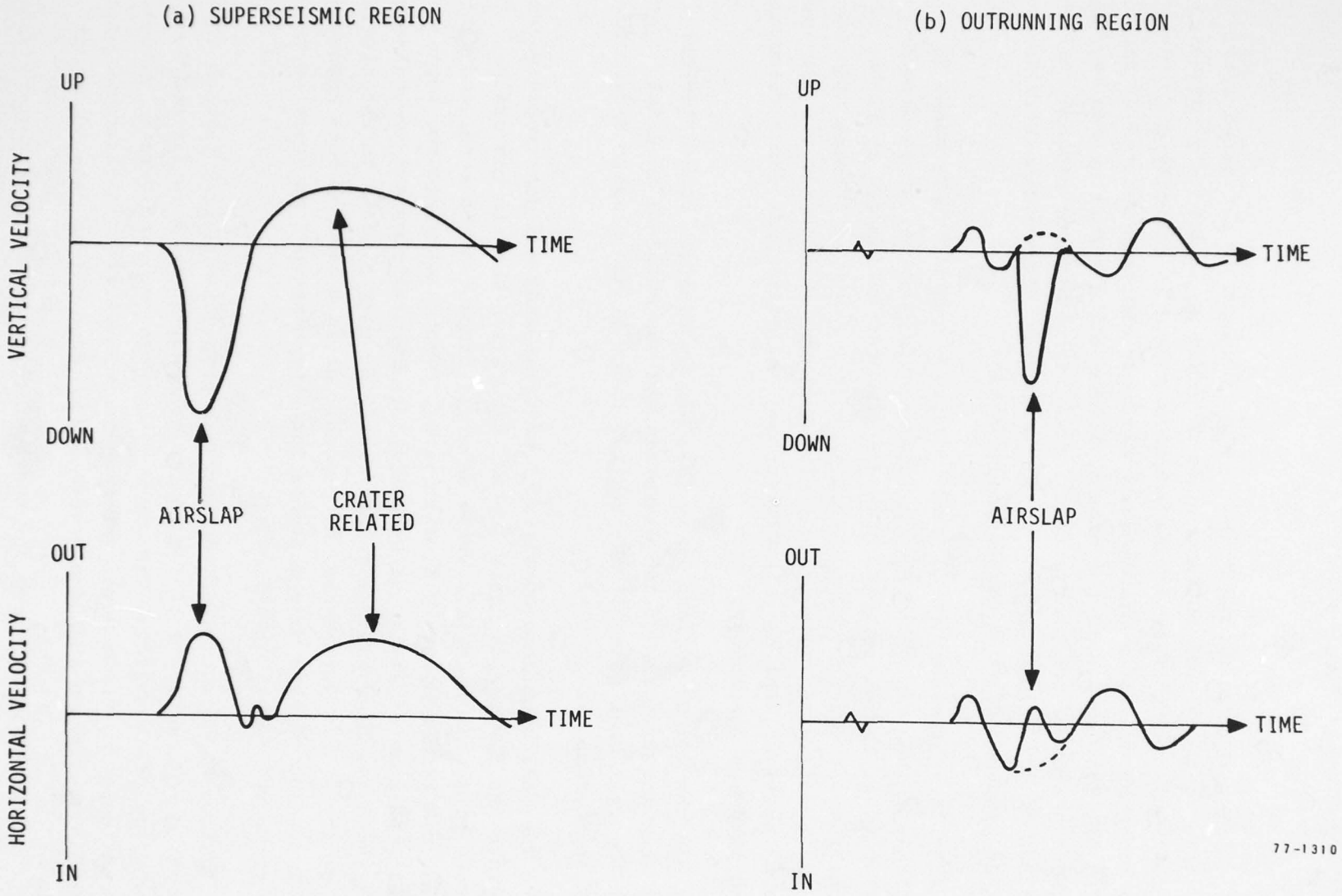

Figure 7. Typical Waveforms for Cratering Bursts

through the highly-energy-absorbing earth medium and therefore faces similar attenuation whether the initial energy deposition was by air shock or direct coupling.

5.3 Summary of Important Effects

Table 2 summarizes some of the important phenomenological characteristics of nuclear detonation ground shock. While not all inclusive, the table lists perhaps the minimum of factors to be accounted for in the ground shock estimation process.

6. SYSTEM REPRESENTATION

The purpose of this subsection is to enumerate the various assumptions and simplifications made by the ground shock estimation community in arriving at a mathematical representation of the ground shock processes. The source of the material to be presented is primarily References 4, 5, and 6, and conversations with various members of the community. Table 3 summarizes the topics in this section. While all of the listed elements may not apply to a particular model or application, they are the common assumptions of the ground shock system representation. In general, the key assumptions about mathematical representation of the ground shock process can be conveniently divided into three areas:

a) assumptions about energy input;
b) assumptions about the geological profile; and
c) assumptions about material behavior.

The assumptions about energy input sometimes differ depending on whether the problem under consideration is an a priori ground motion estimate or an a posteriori comparison of computed ground motions and field data. For an a priori prediction the following assumptions about energy input are generally made:

a) that the detonation is axisymmetrical in directions parallel to the ground surface;

b) that the airblast loading waveform is ideal and expressible as an analytic function of weapon yield (or HE charge size), height of burst, distance to the ground zero, and time;

Table 2. Summary of Important Characteristics

REGION	IMPORTANT CHARACTERISTICS
• CRATER	• HIGH TEMPERATURE AND PRESSURE • CHANGE OF PHASE OF MATERIALS • SHEARING FRACTURE AND SPALL • RESIDUAL MATERIAL STRENGTH • HIGH STRAIN RATES • LARGE DISPLACEMENTS • RADIATION COUPLING
• SUPERSEISMIC AIRBLAST	• AIRSLAP • LAYERING NEAR SURFACE • LOW FREQUENCY DIRECT INDUCED MOTION • NON-LINEAR, ENERGY ABSORBING CHARACTERISTICS OF EARTH MEDIUM
• SURFACE OUTRUNNING	• SURFACE AND INTERFACE WAVES • DEEP LAYERING • GROUND ROLL • NON-LINEAR, ENERGY ABSORBING CHARACTERISTICS OF EARTH MEDIUM

Table 3. Summary of Key System Representation Elements

- ENERGY INPUT
  - AXISYMMETRICAL OUTPUT
  - IDEAL AIRBLAST-INDUCED EXPRESSABILITY
  - IDEAL DIRECT-INDUCED INITIALIZATION
    - HYDRODYNAMICS
    - SOLID MECHANICS
- GEOLOGICAL PROFILE
  - AXISYMMETRICAL GEOLOGY
  - DISCRETE LAYERS
  - HOMOGENEOUS LAYERS
- MATERIAL BEHAVIOR
  - CONTINUUM
    - EQUATIONS OF MOTION
    - CONSERVATION OF MASS
    - CONSERVATION OF ENERGY
    - STATE/CONSTITUTIVE EQUATIONS
      - STICK
      - CAP
  - SINGLE-PHASE
  - RATE-INDEPENDENT
  - ISOTROPIC

c) that the direct-induced energy is a known fraction of the weapon yield and can be expressed in terms of a specified initial velocity and internal energy field.

The assumptions generally made about the geological profile are:

a) that axisymmetry exists around the ground zero of the weapon;

b) that the geological profile can be represented by a series of layers whose boundaries are sharp and parallel to the ground surface;

c) that the material in any one layer is homogeneous.

The common assumptions about material behavior are:

a) that the materials behave as a continuum;

b) that the materials can be represented locally as possessing a single phase;

c) that the material behavior is rate-independent;

d) that the material behavior is isotropic.

Overall, the general assumptions about energy input and geological profile lead to a geometric representation of the ground shock system such as is shown in Figure 8, which is taken from Reference 7. This geometric representation is usually referred to as the Site Idealization.

The assumption that materials behave as a continuum reduces the ground motion estimation process to the simultaneous solution of a set of partial differential equations representing:

a) the equation of motion for the ground;

b) the equation of continuity expressing conservation of mass;

c) the equation expressing energy conservation;

d) the equation of state and/or the constitutive equations for the materials,

subject to the appropriate initial and boundary conditions.

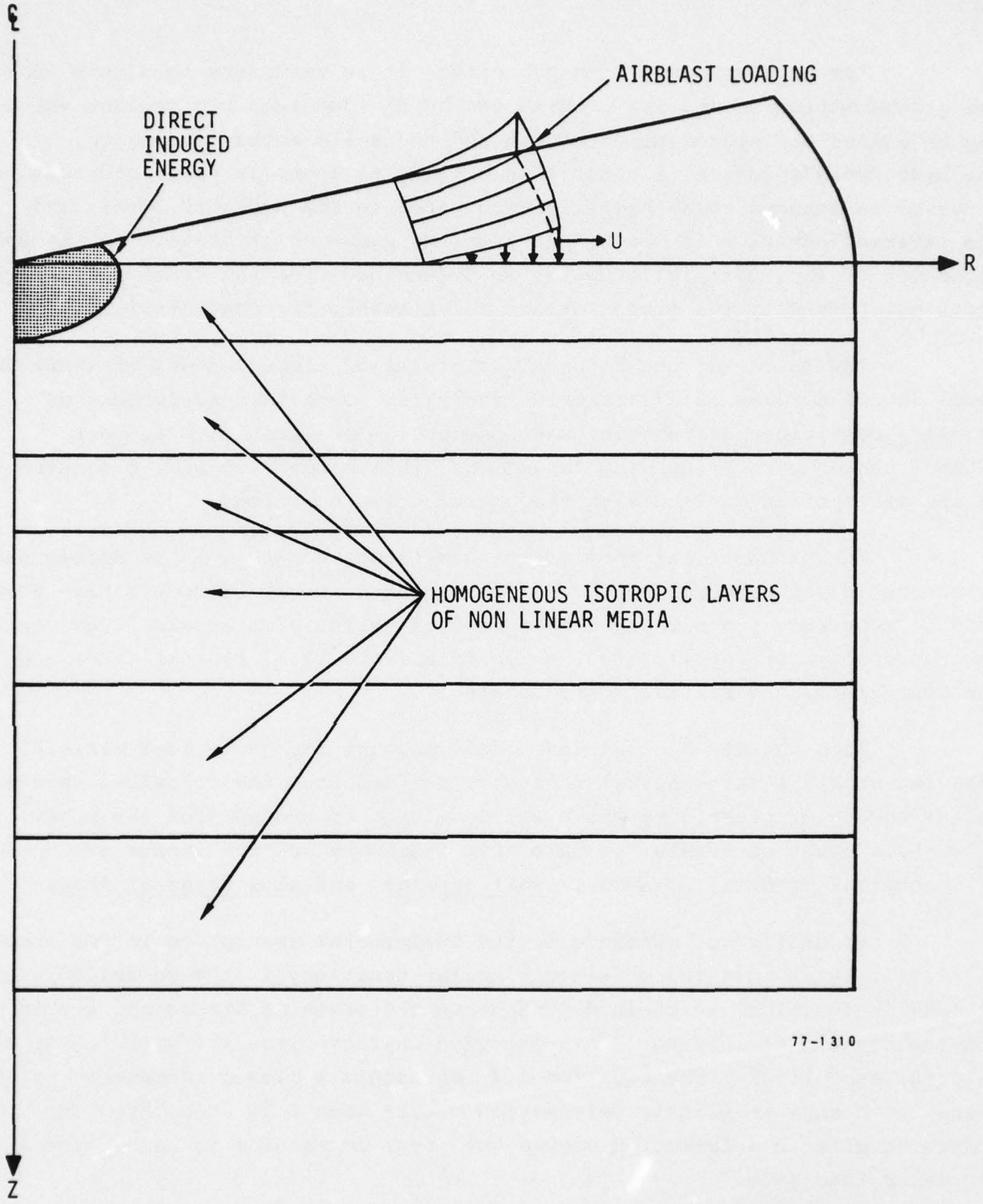

Figure 8. Geometric Representation of Ground Motion Problem

For problems involving cratering, it is customary to assume that the ground motion estimation problem can be divided into two regions which may be called the hydrodynamic region and the solid mechanics region. In the hydrodynamic region, a material's ability to transmit shear and tensile stresses is assumed to be negligible compared to the pressure level, and the material behavior is determined from the equation of state. In the solid mechanics region, material behavior is determined from the constitutive equations which specify the stress/strain relationship for the materials.

The choice of the mathematical forms of the equations of state depends on the details of a particular analysis. Certain descriptions of boundary conditions or behavior make one choice preferable to another. Rather than enumerate the many variations, this discussion will concentrate on the assumptions dealing with the constitutive equations.

The mathematical form of the constitutive equations is determined by the choice of material model. A fairly large number of models have been used to represent the mechanical behavior of geologic materials. However, the currently most popular are the Hybrid Elastic Ideal Plastic (EIP) and the General Elastic Plastic (CAP) models.

Both the EIP and the CAP models account for geological material behavior within a mathematical framework derived from the so-called incremental theory of plasticity which was developed to account for the behavior of certain types of metals. Within this framework are the innate assumptions of isothermal material behavior, small strains, and slow rates of flow.

According to Reference 6, the fundamental assumption in the theory of plasticity is that there exists a scalar function, f (the so-called yield or loading function) which is dependent on the state of stress and strain and the history of loading. This function characterizes the yielding of the material as follows: the equation f=0 represents a closed surface in stress space; no change in plastic deformation occurs when f is less than zero; change in plastic deformation occurs when f=0; no meaning is associated with f greater than zero.

A material is thus defined to be either in an elastic ($f<0$) or a plastic ($f=0$) state. When in a plastic state, the material is defined to be in a condition of loading, unloading, or neutral loading depending on whether the stress increment vector is directed outward, inward, or along the tangent to the loading surface.

A differentiation is made between a so-called ideal plastic solid and a work hardening plastic solid. For an ideal plastic solid, it is assumed that plastic strain is incompressible, that the yield function is of the form: $f=J_2'-K^2=0$ (where J_2' is the second invariant of the stress deviator tensor), and that during plastic flow, the time rate of change of plastic strain is linearly proportional to the stress deviation.

For a work hardening plastic solid, the yield function is assumed to be a function of three parameters: the state of stress in the material; the state of plastic strain in the material; and the so-called work hardening parameter which is dependent on the plastic deformation history of the material. The definition of work hardening ensures that during a load-unload cycle the net work done on a material by an external agency will be either zero or positive. This definition has the following consequences: the yield surface and all subsequent loading surfaces will be convex in stress space; the plastic strain increment vector will be normal to the loading surface; and the rate of change of plastic strain is a linear function of the rate of change of stress.

A Hybrid Elastic Ideally Plastic model (typified by the AFWL "Stick" Model) and the General Elastic Plastic (CAP) model have a number of similarities. Both models explicitly consider the compressive behavior of geological materials. The behavior of geological materials in tension is generally extrapolated from the compressive behavior predictions.

Both models also assume that the loading (or failure) surface is a function of J_1 and J_2' (see Figure 9), the first and second invariants of the stress and stress deviator tensors, respectively. The Stick model represents the loading function(s) $f_1(J_1, J_2')=0$ by up to three piecewise linear segments. The Stick model has two failure surfaces to represent the behavior of certain materials. The upper failure surface represents the characteristics of the "virgin" (i.e., non-blast-loaded) material. The lower failure

(a) HYBRID ELASTIC IDEALLY PLASTIC MODEL

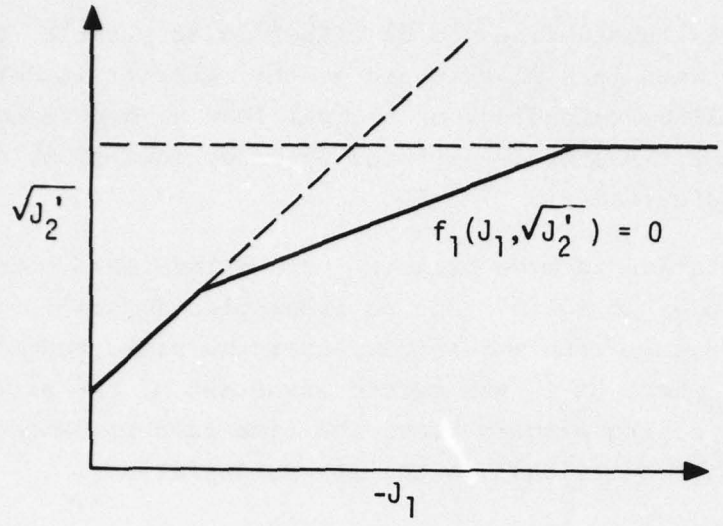

(b) GENERAL ELASTIC PLASTIC (CAP) MODEL

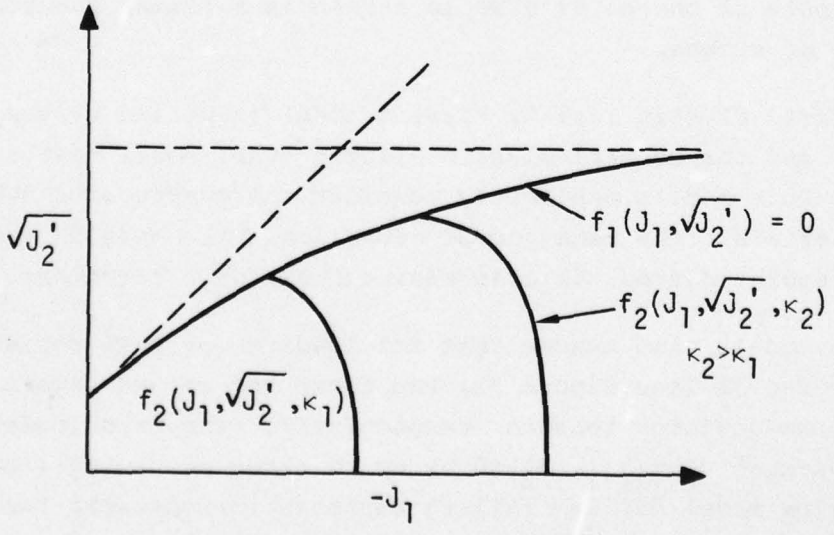

77-1310

Figure 9. Form of Loading Functions

surface represents the condition where the material has been fractured by some initial loading (say an early airblast-induced pulse) so that subsequent waves pass through broken rather than "virgin" material. This behavior is commonly referred to as the "falling failure surface." According to Reference 8, the CAP model represents the loading function as the sum of a linear function of J_2' and the exponential function of J_1. The CAP model also introduces the second loading surface $f_2(J_1, \sqrt{J_2'}, \kappa)=0$ shown in Figure 9. This surface is represented by an ellipse of constant eccentricity and the work hardening parameter κ is equal to the plastic volumetric strain.

The models handle the non-linear bulk and shear moduli in somewhat different fashions. The "Stick" model assumes that the unloading bulk modulus is a constant no matter what the state of isotropic compression, and assumes that the loading modulus is a piecewise linear function of J_1. The "Stick" model also assumes that the ratio of the shear modulus to the bulk modulus is a constant that depends on whether the material is loading or unloading (i.e., that Poisson's ratio depends on whether the material is loading or unloading).

The CAP model assumes that the bulk modulus is an exponential function of J_1 (the first invariant of the stress tensor) and κ (the hardening parameter). The shear modulus is assumed to be an exponential function of J_2', the second invariant of the stress deviator tensor, and κ.

A further difference arises because the assumption of the Stick model, that plastic flow in soils is incompressible, leads to a "non-associative" plastic flow rule, while the assumptions of the CAP model lead to an "associative" plastic flow rule. Drucker's stability postulate (Reference 6) is sufficient, but not necessary, to insure that material models, that use an associative flow rule, satisfy all thermodynamic and continuity requirements for continuum models. This stability insures that all physically realizable initial-boundary value problems are properly posed from a mathematical sense. The non-associated flow rule may not fulfill these requirements, particularly in cases where nearly neutral loading occurs.

7. SYSTEM MEASUREMENTS

The purpose of this subsection is to discuss how the key parameters of the system representation are established and measured. The discussion considers airblast-induced ground motion and is based primarily on

conversations with personnel of the Army Waterways Experiment Station (WES), and the Air Force Weapons Laboratory (AFWL).

The key system parameters are those of the constitutive equations dealing with the site idealization. These parameters are normally established by some combination of in-situ and laboratory test.

7.1 Site Idealization

The site idealization is the geometric system representation by homogeneous parallel layers (see Figure 8). The steps involved in the site idealization process include:

a) Initial Site Characterization;
b) Geophysical Surveys;
c) Geological History;
d) Sample Corings.

The initial site characterization is based on the existing data base of geological profiles in the region of interest. It generally serves to bound final layer definition and as a basis to direct the ensuing measurements.

Geophysical surveys consist of various measurements of seismic velocities along with gravitometric and resistivity measurements. The seismic measurements may be uphole, downhole, and/or crosshole, and include reflection and refraction measurements. The parameters derived from these measurements are seismic velocities, the degree of anisotropy, and material densities. The variation of these parameters with depth further establishes the layer definition.

The geological history provides information on the deep earth properties and on the degree of preloading that may be present in the region of interest.

Sample corings provide direct information on the variation in geological materials with depth. A drilling rig operated by WES has the capability of obtaining approximately five inch diameter corings to depths of about 2,000 feet. These corings provide samples for the laboratory tests to be discussed in the next section.

An additional factor enters into the final definition. This is the pragmatic interaction between the definers of the site idealization and the operators of the ground shock estimation code. This interaction places an upper limit on the complexity of the site idealization due to the physical size of problems that can be handled economically with state-of-the-art computers and codes.

7.2 Establishing Constitutive Equation Parameters

According to Reference 4, constitutive equation parameters are normally established by a combination of in-situ and laboratory data. The procedures being used are somewhat model/site-dependent, but are generally consistent with the flow diagram shown in Figure 10.

The first step in the iterative procedure is to fit the constitutive parameters to the available laboratory test data and the appropriate in-situ test data (geophysical survey data). The next step is to run a computer simulation of an appropriate dynamic in-situ test. The simulation results are then compared with the in-situ test data. If satisfactory agreement is obtained, the model parameters are considered established.

In the event that satisfactory agreement has not been achieved, the next step in the process should be to check if the constitutive model can ever fit the in-situ data. However, sometimes such a check is not possible or can only be done by the principle of exhaustion (mathematical or analysts).

Provided that model revision is unnecessary, the next step is to change the appropriate model parameters. When the selection of parameter values is done by "hand," this step involves the analyst's judgment of model behavior with parameter changes. When the iterative procedure utilizes an automated technique, a modified least squares approach is used to select new parameter values based on minimizing the variance between the computed and in-situ test results. When this step is completed, the process returns to the simulation step.

As can be seen, the estimation of the model parameters is critically dependent on the data derived from the dynamic in-situ and laboratory tests. The nature of these tests will be discussed in the following paragraphs.

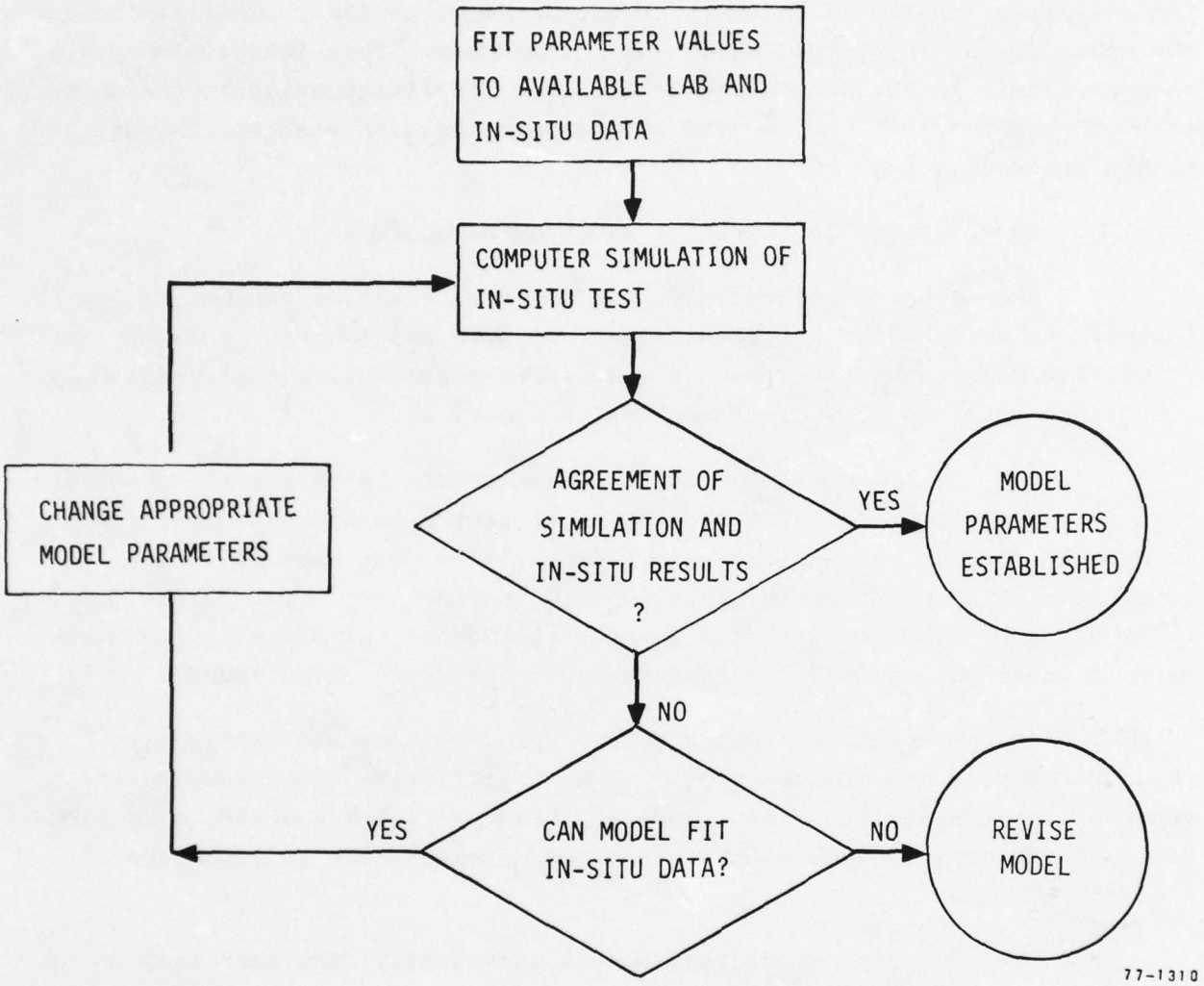

Figure 10. Flow Diagram for Iterative Determination of Model Parameters

7.2.1 Dynamic In-Situ Tests. Reference 9 describes the most current AFWL Cylindrical In-Situ Test (CIST) procedure. The CIST tests are designed to provide experimental data on the dynamic response of near-surface geological materials. The procedure uses an explosive source consisting of PETN primacord that is detonated in a vertical, cylindrical cavity which is in intimate contact with the geological materials. Free-field measurements of acceleration are taken at various ranges from the explosive cavity and at various depths so as to measure ground motions in the principal geological layers at the site under consideration.

Figure 11, taken from Reference 9, shows the cross section of a CIST configuration (CIST 16). The geological profile for this particular site consists of eight layers in the upper 54 feet of the profile.

The 24 inch diameter borehole was lined with steel culvert and filled with racked PETN detonating cord explosive at a density of 5 lbs. per linear foot of hole. Exploding bridgewire detonators are placed such that within a fraction of a millisecond all of the explosive is detonated. Nominal peak cavity pressure is estimated at about 7,000 lbs. per square inch.

Approximately 30 channels of acceleration data are recorded in each test. Both horizontal and vertical measurements are made, but the predominant orientation is horizontal. Cavity pressure transducers are normally installed at the explosive cavity wall to measure the time history of the loading function. Horizontal stress/strain or horizontal stress measurements are made in certain CIST tests.

The pressure transducers are piezoresistive devices that are placed inside filter modules in order to protect them from high pressure spikes and debris. The modules are installed downhole attached to a section of 1/2-inch pipe.

Accelerometers are cast in epoxy canisters which are grouted into the free-field media at the desired locations and orientations. The assumption of axisymmetry at the site is made in laying out the instrument holes since they are not normally aligned along radial gauge lines. Doing so would raise the possibility of gauges shadowing each other.

Backfilling of instrument holes is primarily done with pumpable grout mixed to "match" the soil properties of the appropriate layer. Instrument cannisters are always grouted in and grouting between cannisters

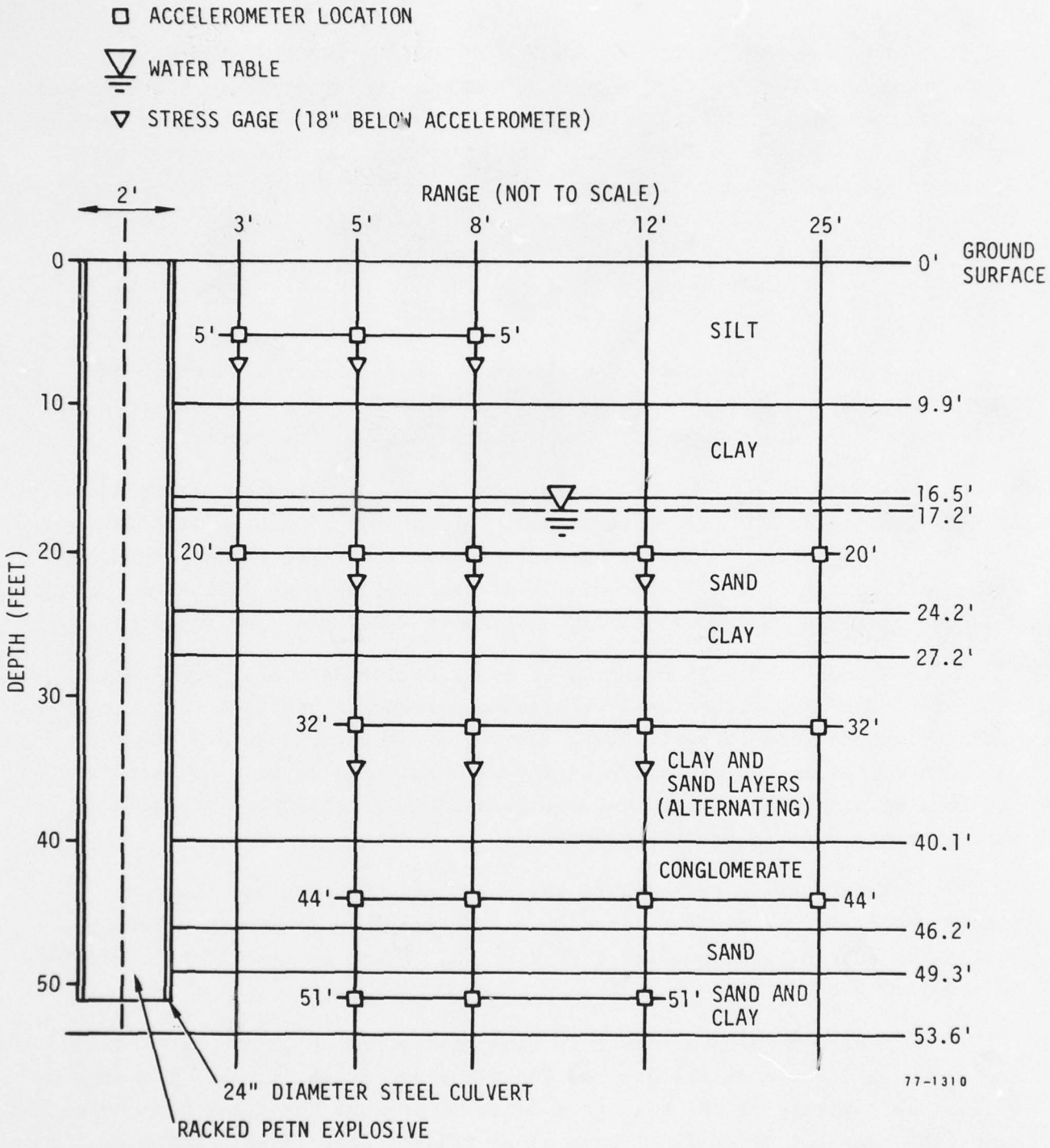

Figure 11. Cross Section of CIST 16

continues to the level where material properties can no longer be "matched" by a grout slurry. Normally this is the upper few feet of the instrument hole where backfilling is done with hand-tamped native material.

Data from accelerometer and pressure transducers are recorded on analog magnetic recording tape. The analog data is then digitized at a frequency comparable to about five times the bandwidth of the recording channel. For dry sites, the digitization rate is 20 kHz. For wet sites, a digitization rate of 100 kHz is normally used. The digitized accelerometer records are corrected for base-line shift and integrated to indicate particle velocity and displacement time histories.

7.2.2 Laboratory Properties Tests. Laboratory properties tests, as typified by those conducted by the U.S. Army Engineer Waterways Station (WES), are divided into three general areas:

1) Classification and Index tests;
2) Composition Tests;
3) Mechanical Properties Tests.

The normal test specimens are vertically oriented cylinders obtained from sample corings. The samples are assumed to be "undisturbed," unless there is visual evidence to the contrary.

Classification and Index tests are concerned primarily with soils. They normally involve the particle size distribution of the sample, the Atterburg limits for clays and silts, and the specific gravity of the sample. These tests primarily define rough mechanical properties and assist in the layer definition for the site idealization process as discussed in Section 7.1

Composition tests determine the relative amounts of soil solids, water, and air in the sample. The tests help determine the "in-situ" density of the sample and aid in interpreting the results of the mechanical properties tests.

Mechanical Properties tests consist of tests of compression and tests of shear. Both static (slow loading) and dynamic tests are performed. Rise times for the dynamic tests are normally of the order of magnitude of milliseconds. Recently developed ultra-fast devices have achieved order-of-magnitude improvement. Two basic types of test apparatus are used by WES in

measuring the mechanical properties of geological materials in compression: uniaxial strain devices and triaxial shear devices. Other equipment includes air overpressure loading and dynamic friction testing apparatus.

According to Reference 10, several assumptions are made in interpreting the results of the mechanical properties tests. Principal among these are:

a) Sample size and loading rates are such that inertial stresses can be neglected in the dynamic tests;

b) Gravity stress due to the weight of the relatively small sample can be neglected;

c) All shear stresses and shear strains are made negligible through the practice of sealing specimens and applying boundary loadings with fluids. This implies a uniform state of vertical stress within the test specimen;

d) Establishing a uniform stress condition in the vertical direction implies that all other states of stress and all states of strain are uniform within the specimen;

e) In-situ overburden stresses can be simulated by applying a preloading to the sample equal to the estimated overburden.

Figure 12, which is taken from Reference 10, illustrates the sample configuration, boundary and loading conditions, and measured responses for the uniaxial strain tests. Dynamic and static tests can be carried out with loading levels up to about 4 Kbars. The principal information derivable from uniaxial strain tests is the constrained modulus which is the local slope of the σ_z vs ε_z curve. Static uniaxial strain tests can also provide data on Poisson's ratio.

Figure 13 illustrates the configuration, boundary and loading conditions, and measured responses for the triaxial shear tests. Dynamic tests can be conducted with confining pressures up to about 12,000 psi while static tests can be conducted with confining pressures up to about 2 Kbar.

The triaxial shear testing apparatus can be used to derive other properties by measuring the radial strain. This, however, involves an

- CONFIGURATION

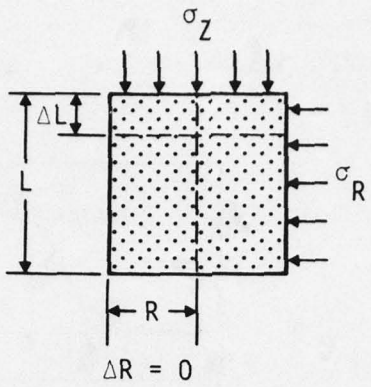

- BOUNDARY AND LOADING CONDITIONS

$\varepsilon_R = \frac{\Delta R}{R} = 0$	IMPOSED
σ_Z (t)	APPLIED AND MEASURED

- MEASURED RESPONSES

$\varepsilon_z = \frac{\Delta L(t)}{L}$	DYNAMIC AND STATIC LOADING
σ_R	STATIC TEST ONLY

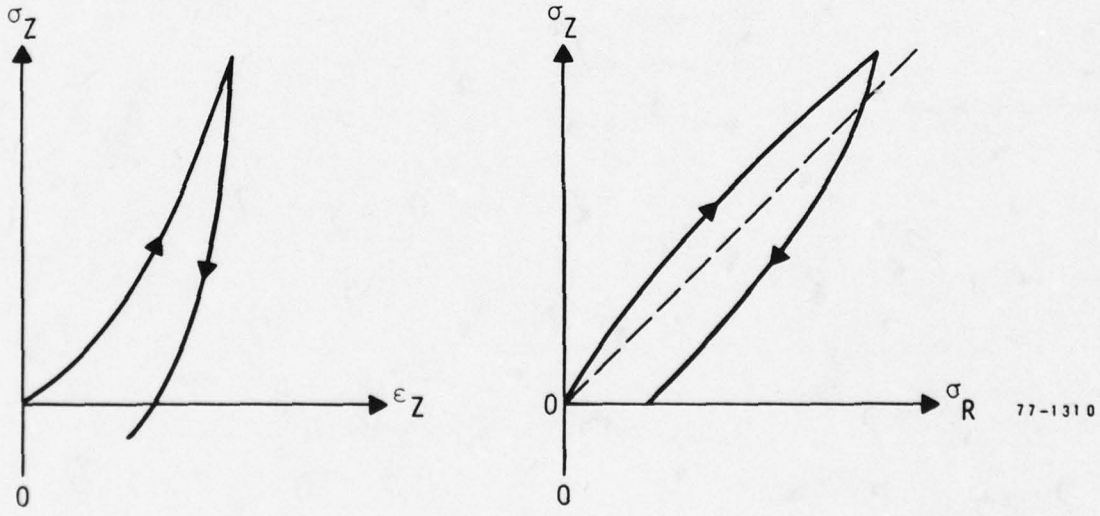

Figure 12. Uniaxial Strain Testing

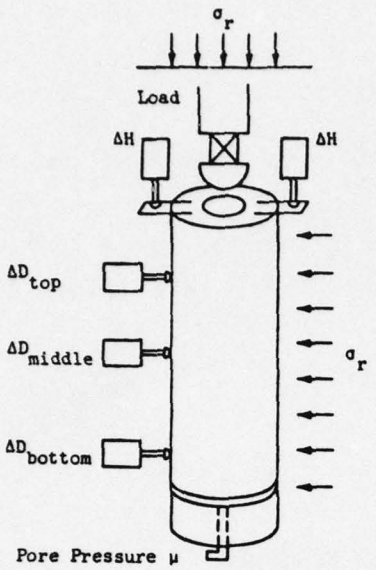

Boundary and Loading Conditions

Hydro

$\sigma_z = \sigma_r$ applied and measured

Shear

σ_r = const applied and measured

Load applied and measured

K°

$\epsilon_r = 0$

Load σ_r applied and measured

Measured Responses

$\epsilon_z = \frac{\Delta H}{H}$

$\epsilon_r = \frac{\Delta D}{D}$

$\sigma_z - \sigma_r = \frac{\text{load}}{\pi D^2}$

σ_r

$P = (\sigma_z + 2\sigma_r)/3$

$\frac{\Delta V}{V_o} = F(\Delta H, \Delta D)$

μ = static only

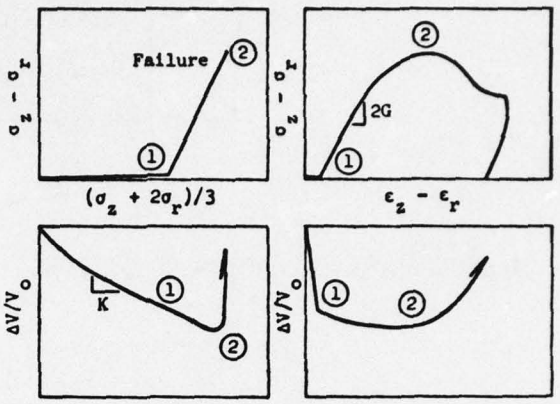

Data plate showing results from a dynamic triaxial shear test

Type Test	Property
Hydrostatic	$K = \frac{\Delta P}{\frac{\Delta V}{V_o}}$
Shear	$G = \frac{\Delta(\sigma_z - \sigma_r)}{2\Delta(\epsilon_z - \epsilon_r)}$
	Failure envelope
K°	$M = \frac{\Delta\sigma_z}{\Delta\epsilon_z}$
	$\nu = \frac{\Delta\sigma_r}{\Delta\sigma_z + \Delta\sigma_r}$

Figure 13. Triaxial Shear Tests

assumption relative to the sample shape during loading. For the isotropic compression test, the uncertainty in sample shape during loading introduces an uncertainty into the value of $\frac{\Delta V}{V}$ equal to the value of the radial strain.

The information that can be derived from the modified triaxial shear test results are: the bulk modulus, from a plot of P vs $\frac{\Delta V}{V}$; the shear modulus, from a plot of $\sigma_z - \sigma_R$ vs $\varepsilon_z - \varepsilon_R$; and Young's modulus from a plot of $\sigma_z - \sigma_R$ vs ε_z. These are all, of course, relative to the static loading condition.

It is normally the practice at WES to report mechanical properties of geological materials in terms of "representative" properties. The construction of these "representative" properties involves the judgment of the soils engineer in choosing properties that "average out" the innate sample-to-sample variations, and in extrapolating static test data to dynamic test data in regions beyond the capabilities of the dynamic testing devices.

8. SYSTEM SIMULATION

Many computer codes have been developed over the years to estimate the free-field ground motion produced by nuclear (or HE) detonation. These codes are all similar in that they treat the geometric representation by a series of finite spatial elements while treating the governing equations in terms of their finite difference analogs.

The codes can be divided into two groups according to whether or not they explicitly treat the hydrodynamic portion of the process for cratering cases. The LAYER code, developed by Weidlinger Associates, appears to be representative of codes that deal with only the solid mechanics portion of the system representation. The AFTON code, developed principally at Applied Theory, Inc., appears representative of codes which address both the hydrodynamic and solid mechanics portions.

The LAYER code (Reference 11) is a Eulerian formulation of the basic equations of the system representation which assumes that transport or convection effects are negligible. This assumption implies small strains and small velocities and is therefore consistent with the basic assumptions of the incremental theory of plasticity (see Section 6).

Under this assumption, the governing continuum equations are formulated such that the stresses and velocities are the only unknown field

variables. The basic equations are the two equations of motion relating the time rate of change of the velocities to the spatial rate of change of the stresses, and four constitutive equations that relate the time rate of change of the stresses to the spatial rate of change of the velocities (i.e., the strain rate components) and the various material moduli needed by the constitutive model(s).

The finite difference analogs are constructed using a staggered grid such as shown in Figure 14, which is taken from Reference 11. In writing these finite difference analogs it is implicitly assumed that velocities and stresses are constant during a time interval and stresses are uniform within a grid cell. Central differences are used for all spatial derivatives, forward differences for the time derivatives in the equations of motion, and backward differences for the time derivatives in the constitutive equations. The sequence of computations for any time step involves first determining the new velocity field from the equations of motion. This field is then used to determine the strain rate components. The strain rate components are then used to obtain the new stresses.

The computational grid elements (see Figure 14) are orthogonal with constant radial mesh size and variable vertical mesh size. Velocities are calculated at the corner of the cells while stresses are calculated at the center of the cells. No slip contact is assumed between cells along layer boundaries. Slip and separation between layers can be modeled by introducing an additional thin layer of material that is very weak in shear and/or tension. As generally implemented, the LAYER code has the capacity to handle in the neighborhood of 12,000 grid cells.

The AFTON 2A code (Reference 12) is an essentially Lagrangian formulation of the basic equations of the system representation. It treats both the solid mechanics and hydrodynamic portions of the ground shock estimation problem. The conservation equations are expressed in their integral form and the finite difference analogs are finite difference equations for conservation of total energy.

The quadrilateral wedge, illustrated in Figure 15, is the basic geometric entity of the finite difference grid mesh used in the AFTON 2A code. Grid point positions and their time derivatives are associated with the vertices of the zones while stress, strain, and internal energy are

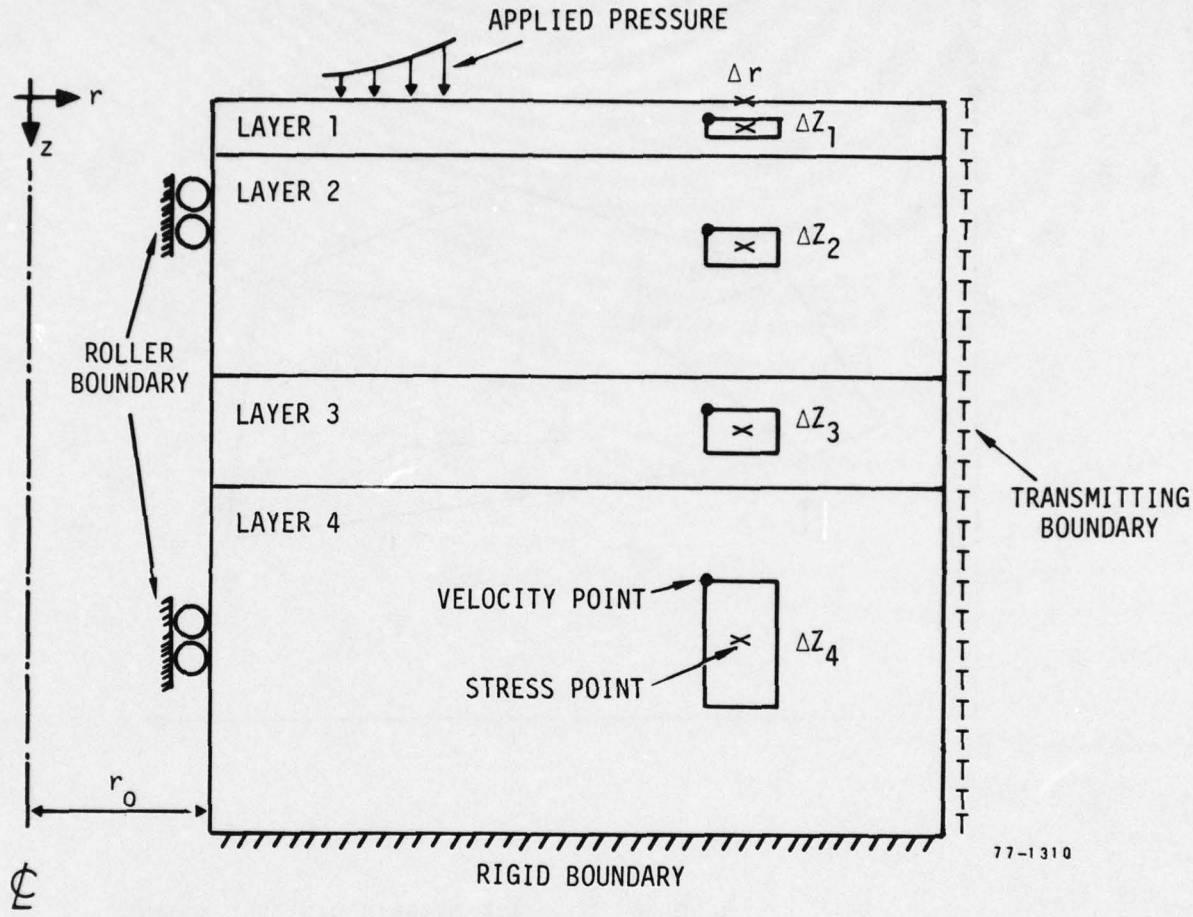

Figure 14. Typical LAYER Code Grid Layout

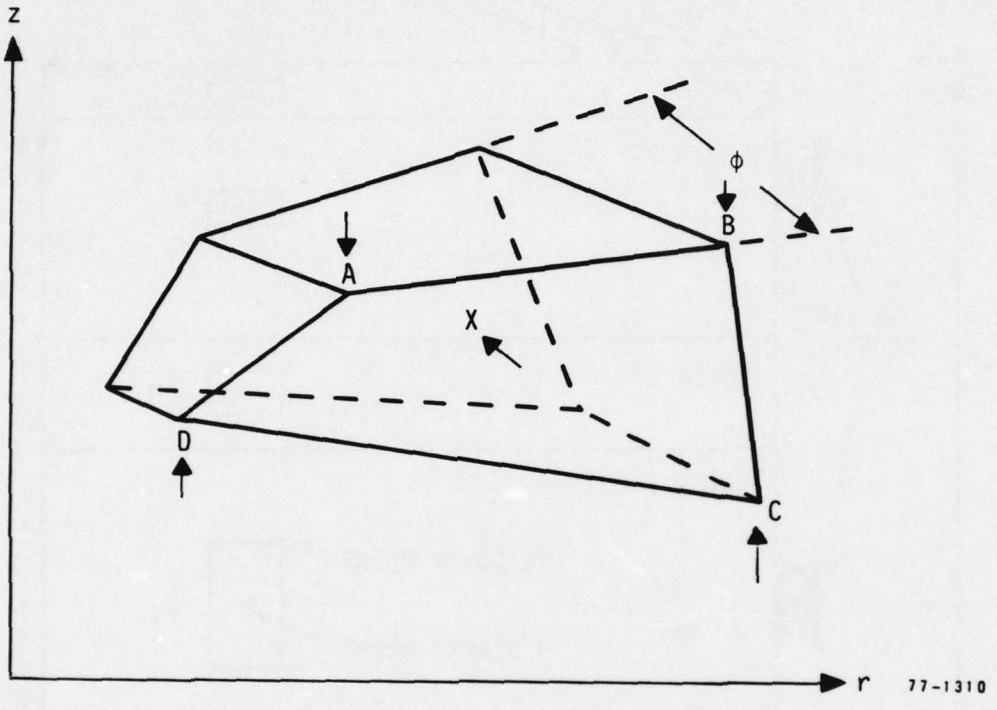

A, B, C, D ARE DYNAMIC VARIABLE POINTS

X IS THERMODYNAMIC VARIABLE POINT

Figure 15. Quadrilateral Wedge of AFTON 2A Code

associated with the center of the zones. Two assumptions are made in the calculation of the zone-centered variables:

a) A material element which initially occupies the region enclosed by the quadrilateral wedge always has the shape of the quadrilateral wedge (i.e., straight lines of mass points deform to straight lines of mass points).

b) Zone-centered variables are constant in value throughout a wedge at any given time, and also change at a constant rate during any particular time-step.

Within the adequacy of these assumptions, the finite difference analog to the First Law of Thermodynamics is exact for the hydrodynamics case and approximate in the solid mechanics case.

Linear and quadratic bulk and deviatoric artificial viscosity terms are introduced into the finite difference analog of the First Law. The purpose of these terms is to "smear out" shock waves over several cells within the computational grid. The artificial bulk viscosity terms are effective in the hydrodynamic portion of the problem while the deviatoric artificial viscosity terms are effective in the solid mechanics portion of the problem.

A user-specified coordinate system, which can range from Lagrangian to Eulerian, is permitted within the AFTON 2A code. When non-Lagrangian coordinate systems are specified, material transport effects are accounted for within the computer model.

In the AFTON code velocities are calculated implicitly from the conservation of momentum equation rather than explicitly as is done in the LAYER code. The calculation of velocity in the AFTON code is based on the concept of a "momentum zone." The momentum zone associated with a mesh point is made up of defined portions of each of the four quadrilateral wedges that show the mesh point as a common vertex. Within the adequacy of the previously mentioned assumption (b), this means that the change in momentum (and therefore velocity) during a time step can be calculated exactly.

The AFTON 2A code is written to be utilized on either CDC or Univac machines. As presently implemented, the AFTON 2A program has the capacity to treat a spatial grid mesh with approximately 12,000 cells.

9. MODEL OF THE GROUND SHOCK ESTIMATION PROCESS

Figure 16 illustrates the authors' understanding of the interactions and interconnections in the present implementation of the ground shock estimation process. The case illustrated considers only airblast-induced ground motion and is based primarily on conversations with various members of the ground shock community.

The process starts with the Problem Definition which is the statement of the type and size of the energy source(s) and the geographical location to be considered. It then branches out to the various steps involved in the System Representation and System Measurement process and finally converges at the input definition and free-field ground shock code used in the System Simulation process.

Three types of flow are shown in the figure: solid lines represent the flow of information from one step to another; the dashed line going from the code back to the layer definition represents constraint imposed by the code on the complexity of the layer definition; and the dotted line going from the representative mechanical properties to the parameter identification step represents an information flow that occurs in some, but not all, problems.

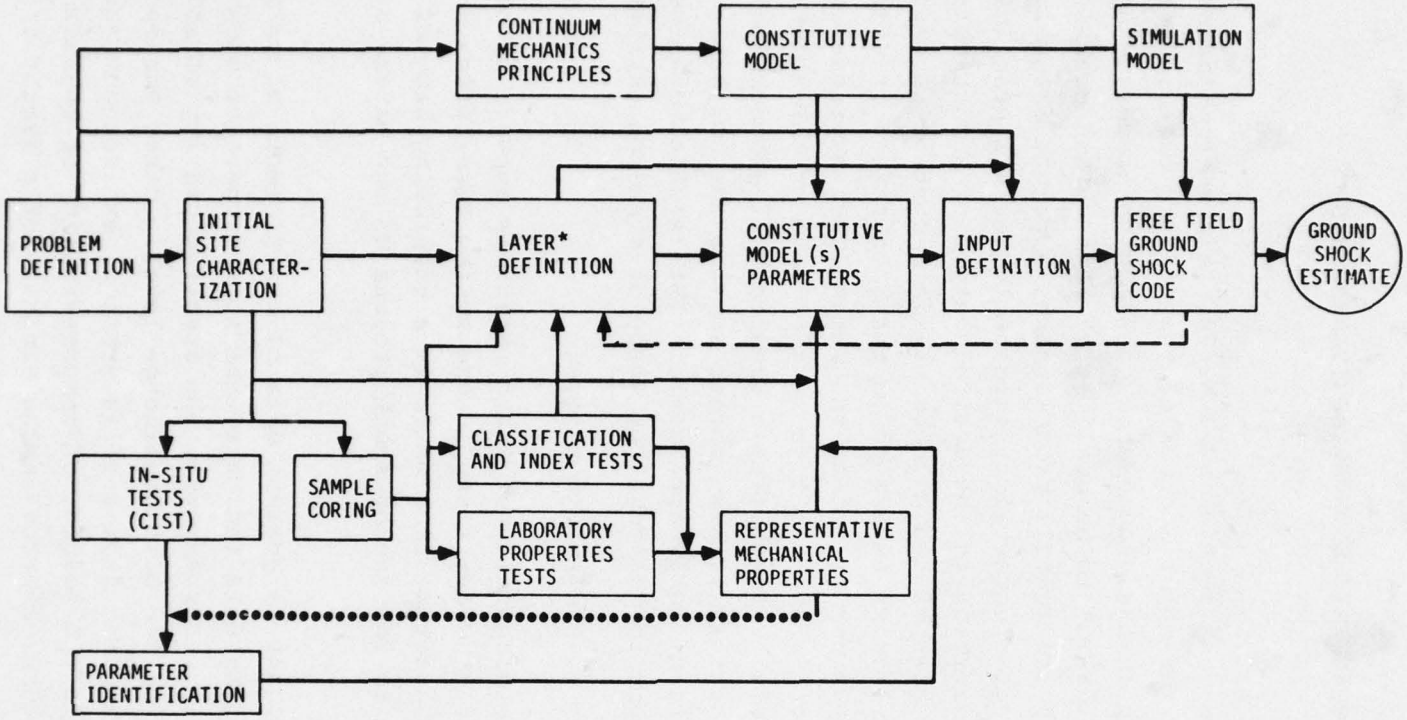

77-1310

Figure 16. Flow Diagram of Ground Shock Estimation Process

SECTION III

QUALITATIVE UNCERTAINTY ANALYSIS

10. GENERAL

Using the previous section as a basis, this section makes a qualitative examination of the major sources of uncertainty that contribute to the overall uncertainty in the ground shock estimation process. Several factors force the examination to be qualitative rather than quantitative. The shear complexity of the overall process makes a priori determination of the effects of a particular uncertainty impossible for all practical purposes. A second consideration is the desired output of a particular ground shock estimation. A factor of two uncertainty in a certain parameter could have a major effect on results expressed in terms of stress or velocity waveforms, but a relatively minor effect if the output were expressed as a shock spectra. Another factor is the relative lack of data on the natural variability of earth materials. Probabilistic treatment of geotechnical engineering problems is a relatively new venture so that the available data base is sparse and not always directly applicable. This section examines the uncertainties as they apply to the four key steps of classical system analysis.

11. UNCERTAINTIES IN SYSTEM DESCRIPTION

The innate heterogeneity of earth materials appears to be one of the two primary sources of uncertainty in the system description area. While this is a well-known characteristic, there is a surprising lack of data that is directly applicable to the ground shock process on the nature and magnitude of heterogeneity.

References 13 and 14 present data on coefficients of variation for some soil properties. The data indicate that some properties show surprisingly little variability. For example, the specific gravity of solids varies by ± 5% when expressed at the 0.95 confidence level. Other parameters, such as initial void ratio and the degree of saturation, exhibit uncertainties in the range of ± 40% while the modulus of compressibility or unconfined compression strength has uncertainties in the vicinity of a factor of two.

Reference 15 points out that the properties of earth materials exhibit spatial correlation. If a soil property at a particular point has a higher (or lower) value than normal, the value a short distance away is also

very likely to be higher (or lower) than normal. For example, Reference 15 describes a site where a vertical correlation distance of 10 ft. exists for the initial void ratio of "bay mud." Horizontal correlation is also indicated--a correlation distance of 180 feet for the index of compressibility of a sand layer; and vertical and horizontal correlations at 17 and 150 ft. respectively for the shear strength of clay material (which had an uncertainty in shear strength of about a factor of 1.6).

Reference 3 presents summary data on the physical and mechanical properties of rock. These suggest that the innate uncertainties are somewhat similar to those mentioned previously for soils--uncertainties in specific gravity of about ± 5% and uncertainties in moduli up to factors of two to three. No data is presented on spatial correlation.

Overall, the available data, while quite sparse and extremely site-dependent, suggests that point-to-point variabilities in material properties can be in the range of factors of 2 or 3. The data also suggests spatial correlations in the range of a few hundred feet in horizontal directions and a few tens of feet in depth.

The degree of reproducibility of weapons effects is the second major source of uncertainty in the system description portion of the ground shock estimation process. For airblast, the important parameters appear to be both peak overpressure and overpressure versus time. For cratering bursts, the important parameters are less clear but appear to be related in an approximate manner to crater volume (Reference 16).

Reference 2 states that nuclear peak overpressure at a given range from ground zero can be predicted, with confidence, to within plus or minus a factor of two. This estimation appears overly conservative for the case where the height of the burst is known and no precursor is formed. In the peak overpressure range of 10 to 1000 psi, an uncertainty at the 0.95 confidence level of plus or minus a factor of 1.2 appears more appropriate. The reproducibility and predictability of the waveform is more difficult to estimate. The data in Reference 17 suggests an uncertainty of about a factor of two in the overpressure at a given range.

For cratering bursts, it is difficult to separate the causes of uncertainties in crater volume. These uncertainties are due to the innate heterogeneous nature of earth materials and the uncertainties in weapon energy

partition and energy coupling. Overall, the data presented in Reference 2 suggests that crater volumes can be predicted within a factor of 2.5 to 3.

In summation, the uncertainties in airblast effects and the heterogeneous nature of earth materials combine to lead to estimated uncertainties in the vertical near-surface motion in the superseismic region of a factor of about 1.2 for peak acceleration and a factor of about 1.5 for peak velocity. These estimates are roughly consistent with the data in Reference 1. While similar estimates are not possible at this time for the outrunning region or for cratering bursts, there is no reason to believe that the uncertainties are less than those for the "air slap" case.

12. UNCERTAINTIES IN SYSTEM REPRESENTATION

The basic sources of uncertainty in the system representation portion of the ground shock estimation process are the validity and/or adequacy of the various assumptions and simplifications that were enumerated in Section 6. These types of uncertainties, regarding energy input, geological profile and material behavior, generally are not expressible in terms leading to uncertainties of a factor of such and such but rather must be viewed in terms of their adequacy within the overall problem.

13. UNCERTAINTIES IN SYSTEM MEASUREMENTS

The principal sources of uncertainty in system measurements arise from:

a) the concept of the site idealization with constant thickness horizontal layers exhibiting constant material properties; and

b) the practices and procedures used to derive representative parameters for use in the various constitutive models.

The first source of uncertainty is the innate heterogeneous nature of typical earth materials. The second is the stochastically-heterogeneous nature of earth materials. These combine with measurement errors in the in-situ or laboratory tests, and errors introduced through sample disturbance and/or the release of "locked in" in-situ stresses while drilling for core samples or establishing instrument stations.

It is impossible at this time to estimate the impact of the uncertainties that arise from the site idealization concept. Reference 18, however, provides some insight into the nature of the problem. The study considers probabilistic one-dimensional consolidation in nonhomogeneous soil systems. It concluded that "It appears that there is no simple way to define an 'equivalent' homogeneous soil (one with single-valued "average" soil properties) for the analysis of one-dimensional consolidation in heterogeneous soil systems. The practice may yield results significantly different from the most probable result for the actual stochastically-heterogeneous system." While the applicability of this conclusion to the ground shock estimation process is certainly not direct, this type of result for a problem that is much less complex than the ground shock process points out the potential for systematic errors to arise from the site idealization concept.

The stochastically-heterogeneous nature of earth materials introduces uncertainties in the representative properties derived for the site idealization whether they are based on in-situ or laboratory tests. The available data on properties of earth materials indicates possible spatial correlation. This means that if a particular sample has higher than normal water content, then other samples from the immediate neighborhood may have higher than normal water content.

This implies that a single CIST test, measuring ground motion over a horizontal distance of at most a few tens of feet, may not be measuring representative motions for the particular geology unless the spatial correlation distances are fairly small, say a few feet at most. Similarly, laboratory properties measurements (without the problems of sample disturbance and measurement errors) may not provide representative values if they are based on sample corings that do not account for spatial correlations.

13.1 Disturbance and Measurement Errors in CIST Tests

There is a potential for introducing local disturbances while drilling the explosives cavity or drilling and refilling the instrumentation holes. What may be termed "measurement errors," however, appear a much more likely source of uncertainty in the CIST testing procedures.

Since the fundamental assumption of the CIST testing procedures is that constitutive model parameters can be derived from the measured ground motions, the accuracy of measurement is of prime importance. The major

factors influencing the measurement accuracy appear to be the degree of coupling between the earth materials and the instrument canisters, the frequency response of the instruments, noisy instruments, and the nature and degree of baseline shifts that occur over the duration of data gathering.

The CIST ground motion data presented in References 9 and 19 suggests that noisy instruments and baseline shifts are the principle sources of uncertainty in the current test measurements. Relatively small accelerometer baseline shifts can cause relatively large errors in the velocities estimated from the integration of the accelerometer records.

For example, an uncorrected 20g baseline shift in an accelerometer record with a peak acceleration of about 2000g's would cause an absolute error in velocity of about 6 ft/sec after 10 milliseconds of integration and 12 ft/sec after 20 milliseconds of integration. This magnitude of error is particularly significant in the latter portions of the velocity waveforms. However, the influence of potential velocity errors of this magnitude on the accuracy of the derived constitutive model parameters is not known at this time.

13.2 Disturbance and Measurement Error in Laboratory Property Tests

The operations of coring, sampling, sample storage, and specimen preparation all contribute to differences between testing and original field conditions. The soil properties that appear to be most frequently influenced by sample disturbances are:

a) Initial state of stress;
b) Initial water content;
c) Shear strength; and
d) Moduli.

The process of coring and sampling often relieves the vertical and horizontal stresses that act on the in-situ material. While the estimated in-situ stresses are applied during the testing process, there is considerable uncertainty as to their values. Vertical stresses can be estimated most reliably, based on sample depth and unit weight and thicknesses of the overburdening layers. Stress history can be examined from odometer stress-strain curves, with the assumption that they have significantly different slopes in the virgin compression region than in the recompression region. However,

References 13 and 14 suggest a large variability (ranging from factors of 1.2 to 5) in the value of the preconsolidation pressure estimated by this procedure. It is not clear whether this variability is due to the innate variability of the materials or due to a sensitivity to testing procedures.

The process of sampling and coring and test specimen preparation may change the level of saturation of the sample from its in-situ value. This may be due to water loss from the sample, to moisture from the boring fluids being absorbed by the sample, or to oxidation effects that produce hairline cracks in the sample. To the extent that a sample's mechanical properties depend on the level of saturation, large bias errors may be introduced into the estimated mechanical properties of the earth material.

The coring and sampling process may reduce or completely destroy chemical bonding or cementation in certain soils. Shear strengths and material moduli derived from stress-strain relationships may thus be underestimated to the degree that disturbed chemical bonding and cementation influence material strength.

The applicability of the laboratory test procedures to a particular test case introduces another potential source of uncertainty. The mathematical analysis of laboratory test measurements involves the imposition of boundary conditions in the conversion of pressure and displacement into stress and strain. Also, static test results are extrapolated to equivalent dynamic test results in pressure regions where equipment limitations preclude dynamic testing. The degree to which the mathematical analyses match the laboratory conditions interposes potential measurement and/or analysis errors.

14. UNCERTAINTIES IN SIMULATION

The principal sources of uncertainty in the simulation portion of the ground shock estimation process are:

1) The application of boundary conditions;

2) The degree to which the finite difference analogs approximate the temporal and spatial derivatives; and

3) The degree to which artificial viscosity terms "smear out" the waveforms and suppress actual high frequency components.

In principle, the uncertainties due to the imposition of boundary conditions can be eliminated by locating the boundaries sufficiently far from the points of interest so that they have no effect during the time period of interest. Similarly, the effects of the finite difference approximations and the artificial viscosity terms can be made arbitrarily small by decreasing the grid mesh size and the time steps used in the calculations.

Unfortunately, the computational speed and storage capacity of state-of-the-art computers limits the number of spatial grid elements for a particular simulation. This places the solutions to the first two sources of uncertainty in opposition since, with a fixed number of grid elements, increasing the physical dimensions of the system to avoid boundary effects increases the size of the spatial grid elements and this degrades the accuracy of the finite difference analogs. Contrariwise, decreasing the size of the spatial grid elements to improve the accuracy of the finite difference analogs may introduce boundary effects into the solution.

Another source of uncertainty arises in the system simulation for materials whose constitutive model shows a stress path dependence. The error in the stress waveforms produced by the finite difference code will cause the various moduli calculated from the constitutive model to be in error. As these moduli are used in calculations later in the simulation, they will introduce further errors.

There is little data on the magnitude of the uncertainties introduced in the simulation portion of the ground shock estimation process. Reference 20, however, considers a layered, elastic geology with physical dimensions in the range of those normally encountered in HE simulation tests (i.e., horizontal distances of 600 to 800 feet and depths of 300 to 600 feet).

Two cases are analyzed in Reference 20:

1) A steady state superseismic, elastic, two-layered problem which has a closed form solution for the stresses;

2) A transient, outrunning, elastic, two-layered problem.

Various grid element sizes and aspect ratios are examined for both cases. The effects of the artificial viscosity terms are also considered. For the superseismic problem, the accuracy of the finite difference code

(TOODY) was assessed by comparison with the closed-form solution of the problem. For the outrunning problem, only relative changes in the calculated parameters with changing grid zone size were evaluated.

Figure 17, which is taken from Reference 20, shows a typical comparison of the velocity waveforms calculated by the TOODY code with the waveforms derived from the closed form solution. The time-coordinate is measured from the arrival of the airblast over the point of interest. The "smearing" effect of the artificial viscosity terms is obvious in early times for both the vertical and horizontal motion. Arrival times match reasonably well, however, if they are based on the inflection point of the initial portion of the calculated waveform. The somewhat better fit to the vertical than the horizontal waveform is characteristic of all results given for the superseismic problem.

Zone sizes ranging from 2.5 x 2.5 feet (horizontal x vertical dimensions) to 10 x 10 feet were examined in the referenced study. The general trend was for the adequacy of the fit to degrade with increasing zone size.

Table 4 summarizes the ratios of the peak stresses and velocities calculated with the TOODY code to those obtained from the closed-form solution for two depths: 25 feet, which was half way between the ground surface and the assumed layer interface; and 100 feet, which was 50 feet below the assumed layer interface. As can be seen, the peak vertical components exhibit ratios near unity for all the grid zone sizes considered. The agreement for the peak horizontal components and the shear stresses, however, degrades rather rapidly with increasing zone size.

The effect of artificial viscosity was examined by calculations with the quadratic bulk viscosity coefficient reduced by a factor of 2.5 and the deviatoric artificial viscosity coefficients set to zero. It was found that with lower viscosity coefficients the agreement for the shear stress and the peak horizontal stress and velocity improved but the calculated peak vertical stresses and velocities overshot the closed-form solution. The calculated waveforms also exhibited high frequency oscillations with frequency a function of the zone size and the sound speed of the materials.

There is no closed form solution to the outrunning problem and therefore the reported ratios showing the effects of grid zone size are referenced to the results obtained with 2.5 x 2.5 foot zone size. Waveform data

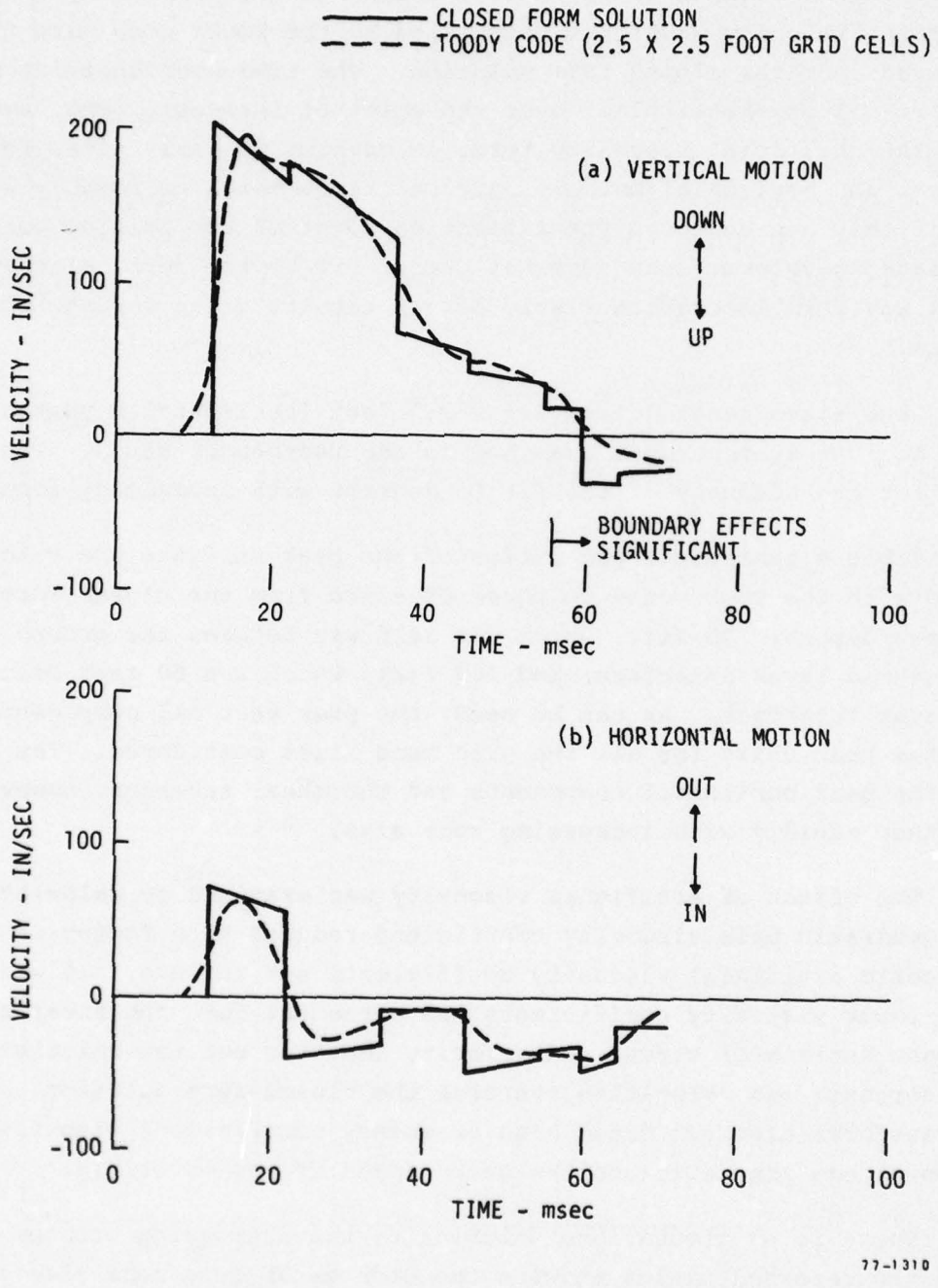

Figure 17. Typical Comparison of Velocity Waveforms/Superseismic Problem/ 25-Foot Depth

Table 4. Comparison of Peak Stress and Velocity Components, Superseismic Problem

ZONE SIZE (FT)	RELATIVE NUMBER OF GRID CELLS TO TARGET POINT	[FINITE DIFFERENCE STRESS] / [CLOSED FORM STRESS]			[FINITE DIFFERENCE VELOCITY] / [CLOSED FORM VELOCITY]	
		VERTICAL	HORIZONTAL	SHEAR	VERTICAL	HORIZONTAL
25 - FOOT DEPTH						
2.5 X 2.5	1.000	0.99	0.86	0.93	0.97	0.90
5 X 5	0.250	0.98	0.82	0.80	0.95	0.77
10 X 5	0.125	0.96	0.77	0.75	0.93	0.70
10 X 10	0.063	0.97	0.73	0.73	0.91	0.53
100 - FOOT DEPTH						
2.5 X 2.5	1.000	0.92	0.88	0.92	0.92	0.89
5 X 5	0.250	0.91	0.79	0.80	0.91	0.77
10 X 5	0.125	0.88	0.71	0.72	0.87	0.66
10 X 10	0.063	0.88	0.64	0.67	0.90	0.61

is presented for depths of 20 feet (10 feet above the layer interface) and 50 feet (20 feet below the layer interface) and at 250, 400 and 500 feet from ground zero.

For the 250-foot range, where the waveforms are dominated by the local airblast-induced motions, the effects of increasing zone size are generally similar to those shown in Table 4 for the superseismic problem. The vertical components show a slower degradation with increasing zone size than do the horizontal components and shear stresses.

Table 5 summarizes the effects of zone size on the peak stresses and velocities at the 500 foot range, where the outrunning motions dominate the airblast-induced motions. For this type motion, the degree of degradation of peak stresses and velocities is similar to that for the superseismic problem, but here the horizontal components degrade less rapidly than the vertical components and shear stress.

Overall, Reference 20 indicates that the TOODY finite difference code may systematically underpredict peak horizontal stress and velocity components and shear stress in problems where airblast-induced motions dominate the waveforms. The results also indicate that the peak vertical stress and velocity components may also be systematically underpredicted in cases where outrunning motions dominate the waveform.

It would be overly simplistic to assume that these conclusions are directly applicable to other finite difference codes or to problems involving multiple layers and inelastic behavior. It is worth noting, however, that with the 2.5 x 2.5 grid cell size about 28000 grid cells were used in analyzing the superseismic problem and about 48000 in the outrunning problem.

15. ESTIMATED DEGREE OF UNCERTAINTY IN MODEL ELEMENTS

Table 6 summarizes the estimated degree of uncertainty, the type of uncertainty, and the principal source of the uncertainty for each of the elements of the ground shock estimation process as illustrated in Figure 16. Degree of uncertainty is expressed as low, moderate, or high based on the authors' estimates of the magnitude of the uncertainties. The estimate reflects impact within the element and potential impact as the uncertainties are propagated through succeeding elements of the process.

Table 5. Comparison of Peak Headwave/Refracted Wave Components, Outrunning Problem, 500-Foot Range

ZONE SIZE (FT)	RELATIVE NUMBER OF GRID CELLS TO TARGET POINT	[PEAK STRESS] / [PEAK STRESS (2.5 X 2.5)]			[PEAK VELOCITY] / [PEAK VELOCITY (2.5 X 2.5)]	
		VERTICAL	HORIZONTAL	SHEAR	VERTICAL	HORIZONTAL
20 - FOOT DEPTH (HEADWAVE)						
2.5 X 2.5	1.00	1.00	1.00	1.00	1.00	1.00
5 X 2.5	0.50	0.88	1.00	0.88	0.89	1.00
2.5 X 5	0.50	0.84	0.91	0.67	0.84	0.77
5 X 5	0.25	0.78	0.88	0.63	0.75	0.85
10 X 10	0.063	0.53	0.63	0.28	0.51	0.58
50 - FOOT DEPTH (REFRACTED WAVE)						
2.5 X 2.5	1.00	1.00	1.00	1.00	1.00	1.00
5 X 2.5	0.50	0.81	0.97	1.00	0.94	1.00
2.5 X 5	0.50	0.76	0.97	1.00	0.85	1.00
5 X 5	0.25	0.70	0.92	0.90	0.82	0.93
10 X 10	0.063	0.41	0.75	0.90	0.58	0.71

Table 6. Estimated Degree of Uncertainty in Ground Shock Estimation Process Elements

MODEL ELEMENT	ESTIMATED DEGREE OF UNCERTAINTY	TYPE OF UNCERTAINTY	SOURCE OF UNCERTAINTY*
● PROBLEM DEFINITION	LOW TO MODERATE	ADEQUACY	
● CONTINUUM MECHANICS	LOW TO MODERATE	ADEQUACY	E.M.
● CONSTITUTIVE MODEL	MODERATE TO HIGH	ADEQUACY	E.M.
● INITIAL SITE CHARACTERIZATION	LOW TO HIGH	ADEQUACY	E.M., D.B., M.E.
● IN-SITU (CIST) TESTS	MODERATE TO HIGH	RANDOM/BIAS	E.M., M.E.
● PARAMETER ID	MODERATE TO HIGH	RANDOM/BIAS	E.M., C.M., CODE, M.E.
● SAMPLE CORING	MODERATE TO HIGH	ADEQUACY/BIAS	E.M., DIST.
● CLASS, AND INDEX TESTS	LOW	RANDOM	E.M., M.E.
● LAB PROPERTIES TESTS	LOW TO HIGH	RANDOM/BIAS	E.M., M.E., DIST., D.B.
● REPRESENTATIVE MECH. PROPERTIES	MODERATE TO HIGH	ADEQUACY/BIAS	E.M., M.E., DIST.
● LAYER DEFINITION	MODERATE TO HIGH	ADEQUACY	E.M., CODE
● CONSTITUTIVE MODEL PARAMETERS	MODERATE TO HIGH	ADEQUACY/BIAS	E.M, M.E., DIST., C.M.
● INPUT DEFINITION	MODERATE TO HIGH	RANDOM/BIAS	E.M., W.E.
● GROUND SHOCK CODE	MODERATE TO HIGH	BIAS	F.D., C.M.

*Sources are: E.M. - Innate Variability of Earth Materials
D.B. - Adequacy of Geological History Data Base
M.E. - Measurement Errors
C.M. - Constitutive Model
Code - Free Field Ground Shock Code
Dist - Sample Disturbances
W.E. - Weapons Effects
F.D. - Finite Difference/Finite Element Approximations

The type of uncertainty and source of the uncertainty vary from element to element. For example, the uncertainty in Problem Definition is of the nature, "Has the problem been adequately defined by the problem poser?" The uncertainties in the Continuum Mechanics Principles and Constitutive Model elements can be characterized, "Are these assumptions adequate to describe the motions of the earth materials under blast loadings?"

The uncertainties re the Initial Site Characterization and the Sample Coring are of the type, "Has there been an adequate geophysical survey?" and "Have there been satisfactory sample corings taken to define the site layering and properties?"

In-Situ (CIST) tests and Laboratory Properties tests have uncertainties that can lead to either random or bias errors. Both are subject to uncertainties arising from disturbances during the drilling and/or sample coring operation. Uncertainties arising from instrument baseline shifts and lack of conformity to the assumed boundary conditions also influence both.

The uncertainties surrounding the Constitutive Model Parameters can be characterized by, "Do these model parameters, that are based on simple stress paths, describe the complex stress paths encountered in the real ground shock environment?" The Ground Shock Code element has a bias uncertainty due to its potential inability to correctly estimate stress paths and shear stresses.

The Parameter ID, Representative Mechanical Properties, Layer Distribution, and Constitutive Model Parameters elements all encounter an uncertainty due to the innate assumption within the ground shock estimation process that may be expressed as "average properties lead to average results."

Overall, the ground shock estimation process has many sources of uncertainty which could lead to the presence of large systematic errors in the ground shock estimate. The majority of these sources arise from the interaction of the innate heterogeneous nature of earth materials with the assumptions made within the various elements of the process. The source of uncertainty that appears to have the greatest potential impact is the validity of the "average properties lead to average results" hypothesis. If this assumption is invalid, the estimation process will always produce a biased estimate as long as there is any uncertainty.

The next significant source of uncertainty arises from the combination of two considerations--(1) the adequacy of the constitutive model, whose parameters are based on simple stress paths, to predict material behavior for the complex stress paths encountered in ground shock motion, and (2) the ability of the ground shock code to correctly estimate these stress paths. The interaction can produce a cascading error effect since a misestimate of the stress paths by the code will cause the constitutive model to predict material moduli that are in error which will in turn cause further error in the ensuing stress paths estimated by the code. Similarly, a misestimate by the constitutive model will cause an error in the stress path produced by the code and the same sequence will follow.

The parameter ID and Representative Mechanical Properties elements have the next highest impact on the estimation process. The potential for bias errors due to sample disturbances and/or instrument baseline shifts has already been mentioned. There is a further source of uncertainty if the average properties hypothesis is valid. This is the degree by which the disturbed or miscalculated properties differ from the true average properties of the site and the impact of this difference on the ground shock estimate.

SECTION IV

QUANTITATIVE UNCERTAINTY ANALYSIS

16. GENERAL

The first objective of this study has been to examine the current ground shock processes and models in order to conceptualize an uncertainty analysis around these elements. With the earlier portions of this report as background, we can now partition various aspects of the problem and apply quantitative methods to develop methodology for establishing uncertainty in the free-field response as a function of the contributory uncertainties. In this section, methods of quantitative uncertainty analysis will be discussed along with the structuring of a number of problems.

17. LINEAR STATISTICAL METHODS

Quantitative statistical models are developed around mathematical models of physical events, processes, etc. If the "event mathematical model" response can be expressed as a linear function of the independent variables, then the statistical model is straightforward. In this case, the general formulation is

$$\{r\} = \{a\} + [C]\{x\} \tag{1}$$

where $\{r\}$ is a vector of responses, $\{a\}$ is a vector of constants and $[C]$ is a matrix of coefficients multiplying the independent variables ℓ_i in the vector $\{x\}$. The elements of $[C]$ are identified as C_{ij}. The expected (mean) value and the covariance of $\{r\}$ are

$$E[\{r\}] = \{\bar{r}\} = \{a\} + [C]\{\bar{x}\}$$

and

$$\text{Cov}[\{r\}] = \left[\sum_r\right] = E[\{r\}\{r\}^T] - \{\bar{r}\}\{\bar{r}\}^T \tag{2}$$

which after substitution and manipulation becomes

$$= [C]\left[\sum_x\right][C]^T \tag{3}$$

where the matrix [Σ] symbolizes the covariance matrix, which in the case of x is

$$\left[\sum_x\right] = \begin{bmatrix} \sigma_{x_1}^2 & \rho_{12}\sigma_{x_1}\sigma_{x_2} & \rho_{13}\sigma_{x_1}\sigma_{x_3} & \cdot \\ & \sigma_{x_2}^2 & \rho_{23}\sigma_{x_2}\sigma_{x_3} & \cdot \\ \text{Symmetry} & & \sigma_{x_3}^2 & \cdot \end{bmatrix} \tag{4}$$

The covariance term $\rho_{ij}\sigma_{x_i}\sigma_{x_j}$ is defined as

$$\text{Cov}(x_i,x_j) = \rho_{ij}\sigma_{x_i}\sigma_{x_j} = \iint_{\text{all } x_i x_j} (x_i - \bar{x}_i)(x_j - \bar{x}_j) f(x_i,x_j) d_{x_i} d_{x_j} \tag{5}$$

where $f(x_i,x_j)$ is the joint probability density function for x_i and x_j. ρ_{ij} is the correlation coefficient and defined by

$$\rho_{ij} = \frac{\text{Cov}(x_i,x_j)}{\sigma_{x_i}\sigma_{x_j}} \tag{6}$$

σ_{x_i} is the standard deviation defined as the square-root of the variance of x_i

$$\sigma_{x_i}^2 = \text{Var}(x_i) = \int_{\text{all } x_i} (x_i - \bar{x}_i)^2 f(x_i) d_{x_i} \tag{7}$$

Scalar representation of the mean and covariance of the response vector are as follows

$$\bar{r}_i = a_i + \sum_{j=1}^{n} C_{ij}\bar{x}_j \tag{8}$$

$$\mathrm{Cov}(r_i, r_j) = \sum_{k=1}^{n}\sum_{\ell=1}^{n} C_{ik}C_{\ell j}\mathrm{Cov}(x_i, x_j) \tag{9}$$

Covariance is an important consideration throughout the problem. It is a measure of the "jointness" of statistical behavior of two or more variables. If, for example, two independent variables x_1 and x_2 behave exactly the same statistically, i.e., when one is large, the other is large in exact proportion, then the two are 100% correlated ($\rho_{12} = 1$) and statistically behave as one random variable. This does not change the mean value as computed in (8) but does significantly influence the variance and covariance. For instance, using (9), if $y = x_1 + x_2$, and if x_1 and x_2 are uncorrelated (independent), then the variance for y is

$$\sigma_y^2 = \sigma_{x_1}^2 + \sigma_{x_2}^2 \tag{10}$$

but if x_1 and x_2 are perfectly correlated

$$\sigma_y^2 = \left(\sigma_{x_1} + \sigma_{x_2}\right)^2 \tag{11}$$

Consequently, in statistical modeling, it is important to identify and measure the correlation in the input variables. In terms of the ground shock problem, it would mean identifying correlation in model parameters.

Seldom are real-world problems truly linear and therefore the use of linear models is limited to those cases where the range of behavior of interest is at least quasilinear. If the problem fits into these limitations, the procedure is as follows:

First, define the vector of responses as a series of functions of the algebraically independent variables

$$\{r(x)\} = \begin{Bmatrix} r_1(x_1, x_2, \ldots, x_n) \\ r_2(x_1, x_2, \ldots, x_n) \\ \vdots \\ r_m(x_1, x_2, \ldots, x_n) \end{Bmatrix} \tag{12}$$

The Taylor's series expansion of this vector is

$$\{r(x)\} = \{r(x_p)\} + \left[\frac{\partial r(x)}{\partial x}\right]_{x_i = x_{ip}} \left(\{x\} - \{x_p\}\right) + 0^+ \tag{13}$$

where

$$\left[\frac{\partial r(x)}{\partial x}\right]_{x_i = x_{ip}} = \begin{bmatrix} \frac{\partial r_1}{\partial x_1} & \frac{\partial r_1}{\partial x_2} & \cdots & \frac{\partial r_1}{\partial x_n} \\ \frac{\partial r_2}{\partial x_1} & \frac{\partial r_2}{\partial x_2} & \cdots & \frac{\partial r_2}{\partial x_n} \\ \frac{\partial r_m}{\partial x_1} & \frac{\partial r_m}{\partial x_2} & \cdots & \frac{\partial r_m}{\partial x_n} \end{bmatrix}_{x_i = x_{ip}}$$

where x_{ip} are reference or mean conditions of the variables x_i around which the expansion takes place.

Ignoring higher order terms, (13) can be rewritten as

$$\{\Delta r\} = \frac{\partial r(x)}{\partial x} \{\Delta x\} \tag{14}$$

Then, using the expressions in (2) and (3) for expected value and covariance

$$\{\overline{r - r_p}\} = \left[\frac{\partial r(x)}{\partial x}\right]\{\overline{x - x_p}\} \tag{15}$$

$$\left[\sum_r\right] = \left[\frac{\partial r(x)}{\partial x}\right]\left[\sum_x\right]\left[\frac{\partial r(x)}{\partial x}\right]^T \tag{16}$$

One of the desirable characteristics of the linear statistical model is the fact that if the x_i variables are normally distributed, the responses are normally distributed. This is true regardless of the presence of correlation. It is also true, but the rule should be used with caution, that regardless of the distributions of the x_i variables, the responses r_j will have a central tendency. In fact if all of the x's were independent with equal impacts on the responses, the distributions for the response variables would tend toward normal distributions.*

If the vector function $\{r(x)\}$ is too nonlinear to ignore the second derivative, some problems can still be solved, but the number of variables must be limited and distribution shapes will not be preserved. For instance,

$$r = a + bx + cx^2 \tag{17}$$

can be rewritten in a Taylor's series form with the expansion taking place around the mean (expected) value of x.

$$r \doteq r(\bar{x}) + (b + 2\bar{x}c)(x - \bar{x}) + 2c(x - \bar{x})^2 \tag{18}$$

$$\bar{r} = E[r] = r(\bar{x}) + (b + 2\bar{x}c)E[x - \bar{x}] + 2cE[(x - \bar{x})^2]$$

$$= r(\bar{x}) + 2c\sigma_x^2. \tag{19}$$

*This discussion makes use of the Central Limit Theorem (see, for example, Reference 21).

$$\sigma_r^2 = \text{Var}[r] = E[(r - \bar{r})]^2 \tag{20}$$

and if x is normally distributed, σ_r^2 becomes

$$\sigma_r^2 = (b + 2\bar{x}c)^2\sigma_x^2 + 12c^2\sigma_x^4 \tag{21}$$

However, if shape characteristics of the density function of r are needed, higher statistical moments must be computed and incorporated into an expansion such as the Edgeworth Series (Reference 22) to obtain the distribution shape. Equation 19 shows that the difference between the mean value of r and the value of r at the mean value of x $[\bar{r} - r(\bar{x})]$ is a function of the variance of x and the second-order derivative of r.

In general, closed form statistical models of any but the simplest nonlinear problems are too complicated for practical computation. Consequently it is suggested that whenever the assumptions of linearity are no longer valid, simulation methods be used. These methods are discussed in the following section.

18. SIMULATION METHODS

Simulation (Monte Carlo) methods are a "brute force" means by which uncertainties in responses, operations, etc., can be computed based on a specific model and a specific set of conditions. The basic procedure is shown in Figure 18. Basically, it is very straightforward and operates on whatever mathematical model is used in the deterministic computation. The biggest difficulties lie in first developing an adequate sequence of random numbers and then shaping and correlating the random numbers according to the behavior of the model parameters. One of the features of the FAST programs (References 23 and 24) was the generation of a set of correlated random numbers which were either normally or lognormally distributed. The objective of the procedure was to move from a vector of uncorrelated variables to a set of correlated variables whose correlations are defined by the covariance matrix [Σ]. The eigenvector matrix of [Σ] then becomes the transformation matrix which multiplies the vector of statistically independent random variables to form a vector of correlated random variables.

Random number generators are available which automatically provide uniform and normally distributed random variables. Lognormal variables are generated by using a normal random variable generator and then transforming

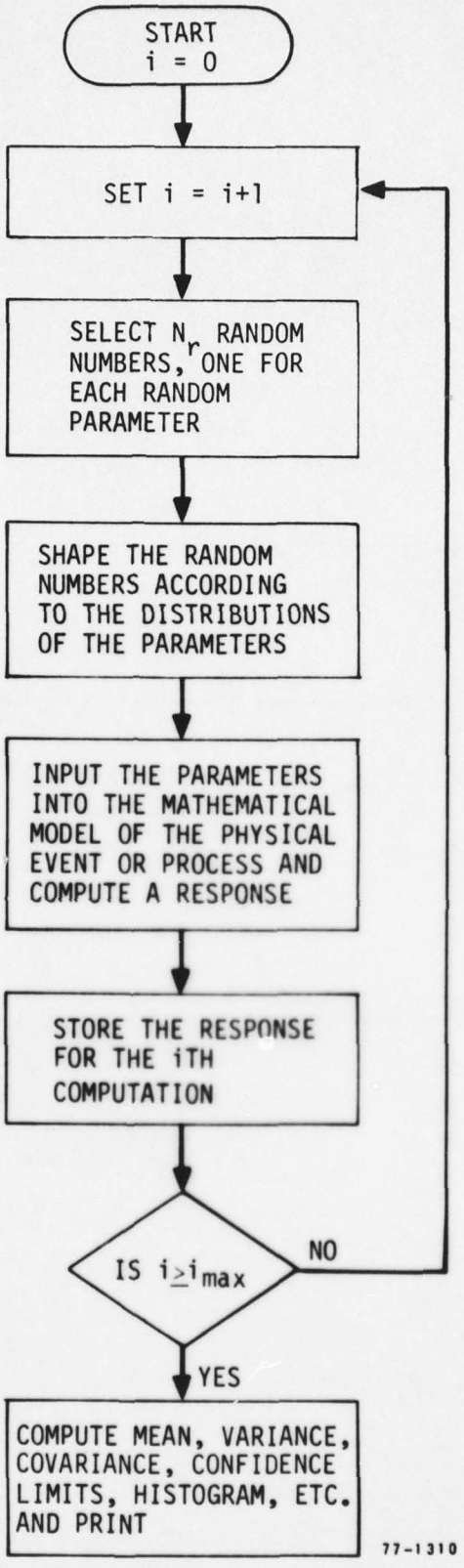

Figure 18. Simulation Procedure

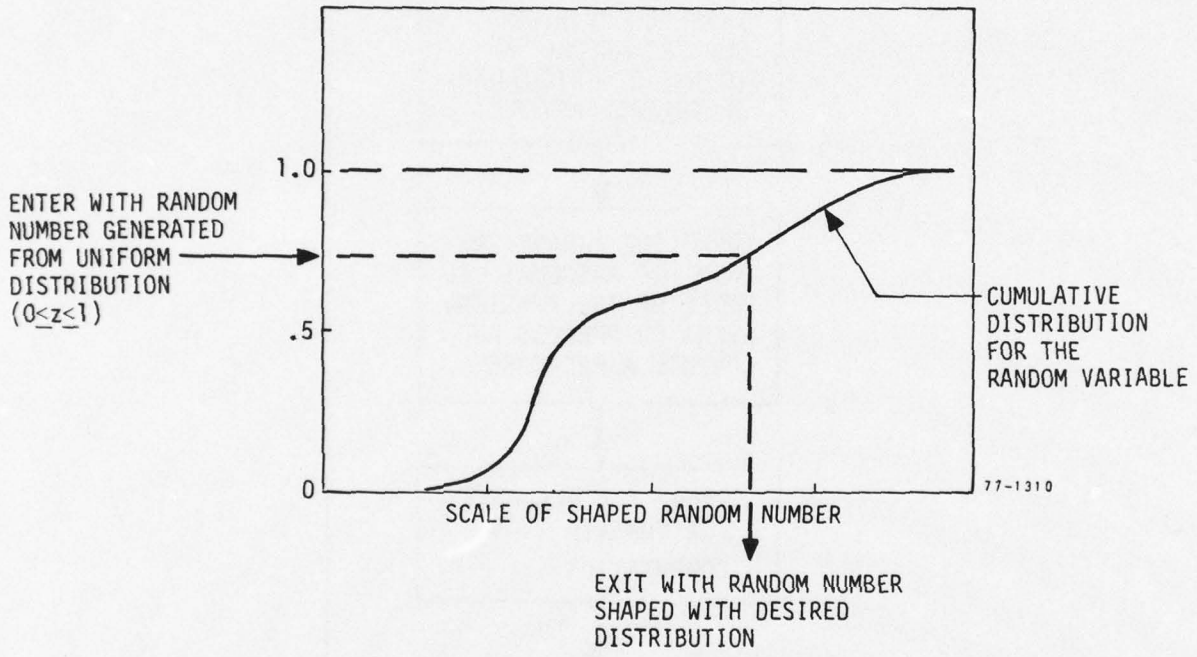

Figure 19. Procedure to Generate Random Numbers for General Distributions

by taking the antilog of the variate. Random numbers of other distributions can be generated by using the uniform random number generator and the cumulative distribution function. The procedure is shown in Figure 19.

The number of cycles in a simulation can depend on funds and/or time. However, if these are not factors, the program should cycle until the confidence limits of the computed mean values fall within satisfactory bounds (for example 1%).

The simulation approach is the most accurate means by which uncertainty can be computed. It does have drawbacks however: it can be very expensive to run; it applies to one set of defined variables only; and it must be rerun completely if any changes are made in any of the inputs.

For the very nonlinear problems which are encountered in evaluating uncertainty in the ground shock problem, simulation is probably the most useful tool. However, careful planning must be exercised to keep both costs and objectives in control.

19. SPECIFIC QUANTITATIVE ANALYSES

The purpose of this subsection is to outline several quantitative analyses that would provide critical insight into the magnitude and effect of some of the uncertainties in the ground shock estimation process. The philosophy behind the selection of the specific analyses is to examine the simplest possible problem that will reflect the impact of the uncertainties on several of the key assumptions within the ground shock estimation process.

A pervading assumption throughout the ground shock estimation process is that "average properties lead to average results." There are two available pieces of evidence that make this assumption suspect. The first of these is the discussion in Section 17 which shows for a simple quadratic relationship, that the average result is not equal to that produced by the average value of the independent parameter, but rather is offset by an amount proportional to the product of the magnitude of the nonlinearity and the degree of uncertainty in the independent parameter. The second is the results of the probabilistic one-dimensional consolidation study (Reference 18) which was discussed in Section 13. This study could find no set of "average" parameters which could reasonably match the expected, or average, result of the Monte Carlo simulations of the problem. Since the free-field ground

shock estimation process is certainly much more complex than either of these examples, the validity of the "average properties lead to average results" hypothesis should certainly be tested.

Two concurrent quantitative analyses appear to be adequate to test the validity of the above hypothesis when applied to the ground shock estimation process. The first of these is a Monte Carlo simulation of wave propagation through a layered half-space whose mechanical properties exhibit point-to-point variability, correlation between parameter values, and spatial correlation. The objective of the analysis would be to determine the level of uncertainty required for the hypothesis to be invalid. The second of the analyses is a statistical analysis of the data available at WES on the physical and mechanical properties of earth materials. The objective of this analysis is to obtain quantitative data on the innate variability of earth materials from geologies that are of interest to the ground shock estimation process and hopefully, to provide estimates of the degree of spatial correlation that exists for the parameters. Upon completion of these two analyses, the validity of the "average parameters lead to average results" hypothesis could be established.

Another quantitative analysis that is suggested is the establishment of the degree to which code assumptions and limitations on number of grid elements affect the ability of the code to predict stress (and velocity) waveforms. This could be done by considering, in the manner of Reference 20, the superseismic elastic two-layer problem which exhibits a closed form solution. This analysis would provide insight into a portion of the uncertainty problem introduced by the interaction of stress path errors with constitutive model errors.

Two other quantitative analyses are suggested to provide insight into the sensitivity of the ground shock estimate to the accuracy with which average properties are established. The first of these analyses would consider the superseismic region and utilize available WES data on a material which shows considerable variation in uniaxial stress/strain paths. Multiple code runs would be made with each run utilizing a different stress/strain path in establishing the parameters of the constitutive model. The second analysis is an examination of the effects of the uncertainties in average properties in the outrunning region. The investigation is a Monte Carlo simulation of an elastic two-layer geology. The effect of the uncertainties

is measured in terms of the uncertainty introduced into the shock spectra for the outrunning region.

The completion of these suggested quantitative analyses would certainly not answer all the questions relating to uncertainties in the ground shock estimation process. They would however provide a basis from which questions related to the validity (or adequacy) of Constitutive Models could be addressed.

SECTION V

SUMMARY OBSERVATIONS AND RECOMMENDATIONS

20. OBSERVATIONS

- The ground shock estimation process is complex and interconnected. In operation, however, it is spatially diffused. Consequently a need exists for communication and close cooperation between the participants.

- Earth materials exhibit large variability in properties, correlation between properties, and spatial correlation between property values.

- Uncertainties resulting from model assumptions and constraints are probably at least as significant as the uncertainties in parameter values (even when the parameters have the wide variability encountered in typical soil situations).

- Difficulties in predicting definitive free-field response increase rapidly with increasing distance between the loading point and the observation point. Uncertainty studies should, therefore, concentrate less on waveform modeling and more on shock spectra for distances beyond the immediate nearfield.

- This study concentrated on airblast-induced problems. Cratering problems exhibit most of the same uncertainty sources and many others and therefore have less predictable waveforms.

- The uncertainty problem has many subsets and should be treated as many specifically defined problems rather than a grandiose simulation.

- The basic (and achievable) objective of the uncertainty studies should be to provide DNA with factors of uncertainty which express the degree of confidence in the various predictions made in the estimation process.

- Another significant source of uncertainty arises from instrumentation errors and biases which influence both the confidence

of prediction and the results with regard to the fundamental behavior of earth materials.

21. RECOMMENDATIONS

- DNA should institute a program to develop more of a "world view" among the various participants in the ground shock estimation process.
- DNA should implement quantitative uncertainty analyses such as those described in Section 19.
- Data base investigations should be instituted emphasizing uncertainties and biases, and their direct and indirect influences on the estimation process.

SECTION VI

REFERENCES

1. Sauer, F.M., G.B. Clark, D.C. Anderson, Nuclear Geoplosics, DASA-1285(IV), Stanford Research Institute, Menlo Park, Calif., May 1964.

2. Crawford, Robert E., Cornelius J. Higgins, Edward H. Bultmann, The Air Force Manual for Design and Analysis of Hardened Structures, Vol I, AFWL-TR-74-102, Air Force Weapons Lab., Kirtland AFB, New Mexico, June 1971 - May 1974.

3. Whitman, R.V., G.B. Clark, Nuclear Geoplosics, DASA-1285(II), Stanford Research Institute, Menlo Park, Calif., May 1964.

4. Defense Nuclear Agency Strategic Structures Division Biennial Review Conference, 8,9,10 February 1977, Stanford Research Institute, Menlo Park, California.

5. Naar, J., Nuclear Geoplosics, DASA-1285(I), Stanford Research Institute, Menlo Park, Calif, May 1964.

6. Fung, Y.C., Foundations of Solid Mechanics, Prentice-Hall, Inc., New Jersey, 1965.

7. Hadala, P.F., "Constitutive Models for Ground Shock Calculations: Lessons Learned from Successes and Failures," Soil Dynamics Division, Soils & Pavements Laboratory, U.S. Army Engineer Waterways Station, Oct. 1976.

8. Sandler, Ivan S., Frank L. DiMaggio, George L. Baladi, "Generalized CAP Model for Geological Materials," Journal of the Geotechnical Eng. Div., Vol. 102, No. GT7, Proceedings of the Am. Soc, of Civil Eng., July 1976.

9. Air Force Weapons Lab, "Cylindrical In-Situ Tests at Selected Nuclear and High-Explosive Test Sites," AFWL-TR-76-209, Air Force Weapons Lab,, Kirtland AFB, New Mexico, Feb. 1977.

10. Jackson, J.G. Jr., "Analysis of Laboratory Test Data to Derive Soil Constitutive Properties," S6916, U.S. Army Eng. WES, Corps of Engineers, Vicksburg, Mississippi, April 1969.

11. Sandler, Dr. I., "Appendix: Brief Description of the LAYER Code," Weidlinger Associates.

12. Schuster, Sheldon H., "The AFTON 2A Computer Code," Air Force Weapons Lab, Air Force Systems Command, Kirtland AFB, New Mexico, Dec. 1972.

13. Diaz-Padilla, J., E.H. Vanmarcke, "Settlement of Structures on Shallow Foundations: A Probabilistic Approach," MIT Dept. of Civil Eng., Report # R-74-9, 1974.

14. Matsuo, Minoru, Reliability In Embankment Design, MIT, Dept. of Civil Eng., Rep. # R-76-33, July 1976.

15. Vanmarcke, E.H., "Probabilistic Modeling of Soil Profiles," Journal of the Geotechnical Eng. Div., Vol 103, No. GT11, Proceedings of the Am. Soc. of the Eng. Div., Nov. 1977.

16. Cooper, Henry F. Jr., "A Review of Ground Motion from Nuclear and High-Explosive Experiments," Strategic Structures Review Meeting, Stanford Research Institute, Menlo Park, Calif., Feb. 1975.

17. Brode, H.L., "Height of Burst Effects at High Overpressures," Defense Atomic Support Agency, RM-6301-DASA, July 1970.

18. Freeze, R. Allan, "Probabilistic One-Dimension Consolidation," Journal of the Geotechnical Eng. Div., Vol. 103, No. GT7, Proceedings of ASCE, July 1977.

19. Amend, Capt. Joseph H. III, Capt. Gilbert W. Ullrich, John M. Thomas, "Have Host Cylindrical In-Situ Test (CIST) Data Analysis and Material Model Report," AFWL-TR-77-81, Air Force Weapons Lab., Air Force Systems Command, Kirtland, New Mexico, Oct. 1977.

20. Higgins, Cornelius, J., David K. Redeen, "Effects of Zone Size, Aspect Ratio, and Artificial Viscosity on the Accuracy of Ground-Motion Calculations with Finite-Difference Codes," AFWL-TR-77-108, Air Force Weapons Lab., Kirtland, New Mexico, Sept. 1977.

21. Cramer, Harald, Mathematical Methods of Statistics, Princeton University Press, Princeton, New Jersey, 1945.

22. Burington, Richard S. and Donald J. May Jr., Handbook of Probability and Statistics, Handbook Publishers, Inc., Sandusky, Ohio, 1958.

23. Collins, J.D., and P.B. Grote, "Ground System Vulnerability Analysis," Technical Report No. 01615-6003-R000, TRW Systems Group, Redondo Beach, Calif., May 1968.

24. Rowan, William H., et al., "Failure Analysis by Statistical Techniques (FAST)," DNA 3336F-1, TRW Systems Group, Redondo Beach, Calif., Oct. 1974.

16. Cooper, Henry F. Jr., "A Review of Ground Motion from Nuclear and High-Explosive Experiments," Strategic Structures Review Meeting, Stanford Research Institute, Menlo Park, Calif., Feb. 1975.

17. Brode, H.L., "Height of Burst Effects at High Overpressures," Defense Atomic Support Agency, RM-6301-DASA, July 1970.

18. Freeze, R. Allan, "Probabilistic One-Dimension Consolidation," Journal of the Geotechnical Eng. Div., Vol. 103, No. GT7, Proceedings of ASCE, July 1977.

19. Amend, Capt. Joseph H. III, Capt. Gilbert W. Ullrich, John M. Thomas, "Have Host Cylindrical In-Situ Test (CIST) Data Analysis and Material Model Report," AFWL-TR-77-81, Air Force Weapons Lab., Air Force Systems Command, Kirtland, New Mexico, Oct. 1977.

20. Higgins, Cornelius, J., David K. Redeen, "Effects of Zone Size, Aspect Ratio, and Artificial Viscosity on the Accuracy of Ground-Motion Calculations with Finite-Difference Codes," AFWL-TR-77-108, Air Force Weapons Lab., Kirtland, New Mexico, Sept. 1977.

21. Cramer, Harald, Mathematical Methods of Statistics, Princeton University Press, Princeton, New Jersey, 1945.

22. Burington, Richard S. and Donald J. May Jr., Handbook of Probability and Statistics, Handbook Publishers, Inc., Sandusky, Ohio, 1958.

23. Collins, J.D., and P.B. Grote, "Ground System Vulnerability Analysis," Technical Report No. 01615-6003-R000, TRW Systems Group, Redondo Beach, Calif., May 1968.

24. Rowan, William H., et al., "Failure Analysis by Statistical Techniques (FAST)," DNA 3336F-1, TRW Systems Group, Redondo Beach, Calif., Oct. 1974.

DISTRIBUTION LIST

DEPARTMENT OF DEFENSE

Assistant to the Secretary of Defense
Atomic Energy
ATTN: Executive Assistant

Defense Advanced Rsch. Proj. Agency
ATTN: TIO

Defense Civil Preparedness Agency
Assistant Director for Research
ATTN: Hazard Eva. & Vul. Red. Div., G. Sisson

Defense Documentation Center
12 cy ATTN: DD

Defense Intelligence Agency
ATTN: DB-4E
ATTN: DB-4C, E. O'Farrell

Defense Nuclear Agency
ATTN: DDST
2 cy ATTN: SPSS
4 cy ATTN: TITL

Field Command
Defense Nuclear Agency
ATTN: FCPR
ATTN: FCTMOF

Field Command
Defense Nuclear Agency
Livermore Division
ATTN: FCPRL

Interservice Nuclear Weapons School
ATTN: TTV

Joint Strategic Tgt. Planning Staff
ATTN: NRI-STINFO, Library

Commandant
NATO School (SHAPE)
ATTN: U.S. Documents Officer

Under Secretary of Defense for Rsch. & Engrg.
ATTN: Strategic & Space Systems (OS)

WWMCCS System Engineering Organization
ATTN: T. Neighbors

DEPARTMENT OF THE ARMY

BMD Advanced Technology Center
Department of the Army
ATTN: 1CRDABH-X
ATTN: ATC-T

Chief of Engineers
Department of the Army
ATTN: DAEN-RDM
ATTN: DAEN-MCE-D

Deputy Chief of Staff for Ops. & Plans
Department of the Army
ATTN: MOCA-ADL

DEPARTMENT OF THE ARMY (Continued)

Harry Diamond Laboratories
Department of the Army
ATTN: DELHD-N-TI
ATTN: DELHD-N-NP

Redstone Scientific Information Center
U.S. Army R&D Command
ATTN: Chief, Documents

U.S. Army Ballistic Research Labs
ATTN: DRDAR-BLE, J. Keefer
ATTN: DRDAR-BLV
ATTN: Technical Library
ATTN: DRDAR-BLT, W. Taylor

U.S. Army Engineer Center
ATTN: DT-LRC

U.S. Army Engineer Div., Huntsville
ATTN: HNDED-SR

U.S. Army Engineer Div., Ohio River
ATTN: ORDAS-L

U.S. Army Engr. Waterways Exper. Station
ATTN: W. Flathau
ATTN: J. Strange
ATTN: L. Ingram
ATTN: G. Jackson
ATTN: Library
ATTN: J. Zelasko

U.S. Army Material & Mechanics Rsch. Center
ATTN: Technical Library

U.S. Army Materiel Dev. & Readiness Command
ATTN: DRXAM-TL

U.S. Army Nuclear & Chemical Agency
ATTN: Library

DEPARTMENT OF THE NAVY

Naval Construction Battalion Center
Civil Engineering Laboratory
ATTN: S. Takahashi
ATTN: R. Odello
ATTN: Code L08A

Naval Postgraduate School
ATTN: Code 0142, Library

Naval Research Laboratory
ATTN: Code 2627

Naval Surface Weapons Center
White Oak Laboratory
ATTN: Code F31

Naval Surface Weapons Center
ATTN: Technical Library & Info. Svcs. Br.

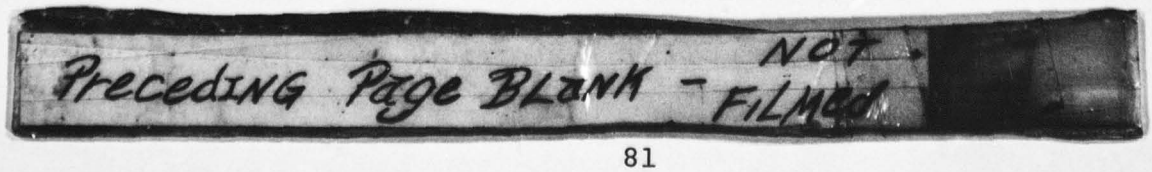

DEPARTMENT OF THE NAVY (Continued)

Naval War College
ATTN: Code E-11

Naval Weapons Evaluation Facility
ATTN: Code 10

Office of Naval Research
ATTN: Coe 474, N. Perrone
ATTN: Code 715

Strategic Systems Project Office
Department of the Navy
ATTN: NSP-43, Technical Library

DEPARTMENT OF THE AIR FORCE

Air Force Geophysics Laboratory, AFSC
ATTN: LWW, K. Thompson

Air Force Institute of Technology, Air University
ATTN: Library, AFIT, Bldg. 640, Area B

Air Force Systems Command
ATTN: DLW

Air Force Weapons Laboratory, AFSC
ATTN: SUL
ATTN: DE, M. Plamondon
ATTN: DES, R. Plamondon

Assistant Chief of Staff
Intelligence
Department of the Air Force
ATTN: INT

Deputy Chief of Staff
Research, Development, & Acq.
Department of the Air Force
ATTN: AFRDQSM

Deputy Chief of Staff
Logistics & Engineering
Department of the Air Force
ATTN: LLEEE

Foreign Technology Division, AFSC
ATTN: NIIS, Library

Rome Air Development Center, AFSC
ATTN: TSLD

Space & Missile Systems Organization
Air Force Systems Command
ATTN: MNN

Strategic Air Command
Department of the Air Force
ATTN: NRI-STINFO, Library

DEPARTMENT OF ENERGY

Albuquerque Operations Office
ATTN: Technical Library

Department of Energy
ATTN: Classified Library

DEPARTMENT OF ENERGY (Continued)

Nevada Operations Office
ATTN: Technical Library

OTHER GOVERNMENT AGENCIES

Central Intelligence Agency
ATTN: J. Ingley

Bureau of Mines
ATTN: Technical Library

DEPARTMENT OF DEFENSE CONTRACTORS

Aerospace Corporation
ATTN: Technical Information Services

Agbabian Associates
ATTN: M. Agbabian

Applied Theory, Inc.
2 cy ATTN: J. Trulio

Avco Research & Systems Group
ATTN: Library, A830

BDM Corporation
ATTN: Corporate Library

Boeing Company
ATTN: Aerospace Library

California Research & Technology, Inc.
ATTN: S. Shuster
ATTN: Library
ATTN: K. Kreyenhagen

Calspan Corporation
ATTN: Library

Civil/Nuclear Systems Corporation
ATTN: J. Bratton

University of Dayton
Industrial Security Super., KL-505
ATTN: H. Swift

University of Denver
Colorado Seminary
Denver Research Institute
ATTN: Security Officer for J. Wisotski

EG&G Washington Analytical Services Ctr., Inc.
ATTN: Library

Civil Engineering Rsch. Facility
The University of New Mexico
ATTN: N. Baum

Gard, Inc.
ATTN: G. Neidhardt

General Electric Company-TEMPO
Center for Advances Studies
ATTN: DASIAC

DEPARTMENT OF DEFENSE CONTRACTORS (Continued)

IIT Research Institute
ATTN: Documents Library
ATTN: R. Welch
ATTN: M. Johnson

University of Illinois
Consulting Services
ATTN: N. Newmark

Institute for Defense Analyses
ATTN: Classified Library

Kaman AviDyne
Division of Kaman Sciences Corp.
ATTN: E. Criscione
ATTN: N. Hobbs
ATTN: Library

Kaman Sciences Corp.
ATTN: Library

Lawrence Livermore Laboratory
University of Calfiornia
ATTN: L. Woodruff
ATTN: Tech. Info. Dept. Library

Lockheed Missiles and Space Co., Inc.
ATTN: Technical Information Center, D/Coll.
ATTN: T. Geers

Los Alamos Scientific Laboratory
ATTN: Reports Library
ATTN: R. Bridwell

Lovelace Biomedical & Environmental Research Inst., Inc.
ATTN: R. Jones

McDonnell Douglas Corp.
ATTN: R. Halprin

Merritt CASES, Inc.
ATTN: J. Merritt
ATTN: Library

Oak Ridge National Laboratory
Union Carbide Corporation
Nuclear Division
ATTN: Civil Def. Res. Proj.
ATTN: Technical Library

Physics International Co.
ATTN: F. Sauer
ATTN: L. Behrmann
ATTN: Techical Library
ATTN: E. Moore
ATTN: J. Thomsen

R & D Associates
ATTN: C. MacDonald
ATTN: R. Port
ATTN: Technical Information Center
ATTN: W. Wright, Jr.
ATTN: J. Lewis
ATTN: J. Carpenter
ATTN: H. Brode
ATTN: A. Latter

R & D Associates
ATTN: H. Cooper

DEPARTMENT OF DEFENSE CONTRACTORS (Continued)

Sandia Laboratories
Livermore Laboratory
ATTN: Library & Sec. Class. Div.

Sandia Laboratories
ATTN: 3141
ATTN: L. Hill
ATTN: A. Chabai

Science Applications, Inc.
ATTN: Technical Library

Science Applications, Inc.
ATTN: D. Maxwell
ATTN: D. Bernstein

Southwest Research Institute
ATTN: W. Baker
ATTN: A. Wenzel

SRI International
ATTN: G. Abrahamson
ATTN: B. Gasten
ATTN: Y. Gupta

Systems, Science & Software, Inc.
ATTN: Library
ATTN: T. Cherry
ATTN: D. Grine
ATTN: T. Riney

Terra Tek, Inc.
ATTN: A. Abou-Sayed
ATTN: Library
ATTN: S. Green

Tetra Tech, Inc.
ATTN: L. Hwang
ATTN: Library

TRW Defense & Space Sys. Group
ATTN: P. Bhutta
ATTN: Technical Information Center
2 cy ATTN: P. Dai

TRW Defense & Space Sys. Group
San Bernardino Operations
ATTN: F. Wong

Universal Analytics, Inc.
ATTN: E. Field

Vela Seismological Center
ATTN: G. Ullrich

Weidlinger Assoc., Consulting Engineers
ATTN: M. Baron

Weidlinger Assoc., Consulting Engineers
ATTN: J. Isenberg

Westinghouse Electric Corp.
Marine Division
ATTN: W. Volz